MINIMAX POLYNOMIAL ECEF TO GEODETIC COORDINATE TRANSFORMATION APPROXIMATIONS

JOHN-OLOF NILSSON

ABSTRACT. Minimax polynomial ECEF to geodetic coordinate transformation approximations are presented, including often preferable n-vector versions and pseudo-code implementations. The approximations provide high accuracy-to-computational-cost tunability and an unprecedented low latency down to an accuracy of $\sim 10^{-5}$m, which is demonstrated in an extensive benchmark. This sets a new standard for coarse and fast ECEF to geodetic coordinate transformations and opens up a new realm of further improvement opportunities and extensions to other geodetic quantities.

1. INTRODUCTION

Cartesian earth-centered earth-fixed (ECEF) coordinate $\{x, y, z\}$ to geodetic coordinates $\{\phi, \lambda, h\}$ (latitude, longitude and altitude, *lla*) or $\{\bar{n}, h\}$ (n-vector and altitude, *nva*) transformations are integral to geodesy and related modeling and simulations and, for many applications, constitute a significant computational cost. The importance of the problem is demonstrated by over 230 publications listed in *Nilsson 2024*, spanning more than 6 decades. However, with its apparent simplicity and many publications, it could be expected to be a closed chapter, but, somewhat surprisingly, transformation methods based on minimax polynomials, the cornerstone of *approximation theory*, are completely lacking. This work fills in this blank and demonstrates how the *complete* transformations can be implemented with minimax polynomials, including often preferable n-vector versions. (See *Gade 2010* for the benefits of the n-vector representation.) This results in high accuracy-to-computational-cost tunability, straight-forward arithmetic-only separable implementations and unprecedented low latency down to an accuracy of at least $\sim 10^{-5}$m, at which the Bowring's method is equally good. The performance is demonstrated in an extensive benchmark of more than 40 methods. This sets a new standard for coarse (relative to the 64-bit numeric limit of $\sim 10^{-9}$m) and fast ECEF to geodetic coordinate transformations (and evaluations) and opens up a new realm of further improvement and extension opportunities.

The improvement opportunities primarily come from the resemblance of the presented approximations to elementary function approximations, for which a vast literature and tool sets exist. For a starting point, see *Muller 2006*. See also the *potential improvement* in the discussion Section 9. The extension opportunities primarily comes from the presented approximations being trivially extendable to other (in addition to latitude and altitude) ellipsoidal z-axis rotation symmetric and xy-plan reflection symmetric or anti-symmetric quantities. The main caveat to it all is that the approximations are only valid for a *preselected* altitude range. The range can be large enough to cover the vast majority of applications, with reasonable performance demonstrated for up to an altitude range of $\sim 500\,000$m.

Significantly beyond that, one has to resort to range splitting, which, on the other hand, is normal for minimax approximations. Further, the presented benchmark is valuable in itself. It is the most extensive benchmark to date and the first benchmark including *nva* transformations, which arguably provides a superior view of the performance of different methods. The results indicate that, in contrast to frequent claims of the opposite; in terms of computational efficiency and for altitude ranges and conversion accuracies reasonable for most applications; there have only been a few marginal improvements beyond *Bowring 1976 + Bowring 1985* method, with *Lin and Wang 1995*, *Olson 1996*, *Wu et al. 2003*, *Fukushima 2006* and *Shu and Li 2010* being noteworthy. Similar conclusions have also been reached in a smaller benchmark *Claessens 2019*.

If you just want a fast polynomial approximation, skip to Table 1 of Section 6 for pseudo-code implementations, then skip to the benchmark results in Figure 1 of Section 7 to select polynomial orders and, finally, get the polynomials from Appendix G. Or take the long route and start in Section 2 for some extended background and notes about novelty and continue with Section 3 where the core range reductions, series expansions and range reconstructions are presented. Section 4 and 5 follows with polynomial approximations of the transformation components and the complete transformations. Section 6 deals with the implementation, Section 7 with the benchmark and Section 8 discusses the benchmark results. Finally, general discussions, caveats and potential improvements are provided in Section 9 followed by final recommendations in Section 10. Many details are referred to the Appendices A-G.

2. BACKGROUND AND NOVELTY

As for most minimax polynomial approximations, there are four fundamental components of the presented transformation approximations; *range reduction*, *series expansion*, *polynomial approximation* and *range reconstruction*; for which some background and further comments about novelty of this work are provided here. First a general comment, there is a significant (former) Soviet Bloc literature on the coordinate transformation subject. This literature is hard to access and has largely been ignored but references are listed in *Nilsson 2024*. However, there is no indication that it contains any transformation methods similar to the one presented here.

The *range reduction* aims at reducing the essentially unbounded ECEF coordinate values to some bounded intervals. For polynomial methods, this essentially entail transforming the ECEF coordinates to the variables of the polynomial approximation. Similar steps are present in most iterative and close-form methods but seldom explicitly recognized as such. Here, the range reduction is split into a commonly appearing, but here implicit, geocentric latitude part, for the approximation derivations, and an explicit but significantly less expensive coordinate normalization, for the actual approximations.

Series expansions are not strictly necessary for polynomial approximation but often helpful in that it provides structure for the later approximation. Polynomial approximation, and particularly series expansions, of ECEF (geocentric latitude) to geodetic coordinate transformations is nothing new. Rather it appears to have been the normal way to transform coordinates in the pre-digital-computers era. Expansions can be found on p40-43 in the standard reference *Helmert 1880*. Helmert, in

turn, cite even older literature. Further, an extensive treatment of series expansions can be found in *Adams 1921*. Moreover, the *Nautical Almanac 1931*, see p718, even contains first order altitude corrections in the conversion from geocentric to geodetic coordinates but, although simple in this case, there is no explicit treatment of how to handle unknown altitude. (The corrections are late provided with some more explanation in *Explanatory Supplement 1961*, see p58.) With the launch of Sputnik 1 on the 4th of October 1957 and the heightened interest and requirements of the space race, numerous publications of altitude dependent series expansions can be found from 1960 and up to 1976 *Berger and Ricupito 1960; Hirvonen 1960; Morrison and Pines 1961; Gersten 1961; Hirvonen and Moritz 1963; Pick 1967; Mikhailov 1967; Pavlov 1968; Getchell 1972; Long 1974; Long 1975; Deprit and Deprit-Bartholome 1975; Sünkel 1976*. However, after the seminal *Bowring 1976* iterative method, they appear to wane in popularity. Some notable exceptions are *Eissfeller 1985; Olson 1996; Turner and Elgohary 2013; Guo et al. 2014; Escapa and Fukushima 2019*. There has also recently been some work on non-altitude dependent expansions *Orihuela 2013; Li et al. 2022; Karney 2023*. However, the series expansions of the literature typically have three fundamental short-comings: 1) They partially rely on inefficient (local) derivative based series expansions. 2) The series variables are often not directly available. 3) The series are only for latitude, whereas altitude is computed with an exact latitude based formula and the approximated latitude. Here novel general series expansions are presented, directly in ECEF coordinate norm and normalized coordinates for latitude, altitude and the n-vector. The series expansions contains no derivatives.

The *polynomial approximation* of the literature methods are, without exceptions, done by truncating the series expansions. This is simple but it is well known in *approximation theory* that this is typically suboptimal. Rather minimax approximations should normally be used. The Remez algorithm for computing such polynomials has been around since *Remez 1934* and the field can be described as well established since the 60s *Fraser 1965*. Hence, it is somewhat surprising that minimax is nowhere mentioned within the over 230 references listed in *Nilsson 2024*. However, there is a simple reason minimax approximations has not been used, so far; the coordinate transformation is not a 1-dimensional problem, making the techniques not directly applicable. On the other hand, closely related Chebyshew polynomials are typically used to describe ephemeris data *Newhall 1988* and it is occasionally encountered in map projections and terrain model, so it is not completely unknown to the geodetic community. Nonetheless, here it is shown how minimax approximations can be used for ECEF to geodetic coordinate transformations. Only (Chebyshev) series which can be truncated with close to minimax performance are truncated. In all other places, optimal minimax approximations are used.

Finally, the *range reconstruction* aim at transforming some intermediate approximated quantities to the final quantities of interest. For most approximation methods this means transforming some quantity, proportional to trigonometric function of the latitude, to the final latitude and altitude, i.e. the range reconstruction come in the form of inverse trigonometric functions. These inverse trigonometric functions are just as much a part of the coordinate transformation as any other part and should be approximated with suitable accuracy. Most likely, this is occasionally done in practice but with some rare exceptions *Toms 1996; Toms 1998; Zanevičius*

and Keršys 2010 this is not discussed, despite the range reconstruction making up half the computational cost (as will be shown) and suitable approximations being readily available since at least the 50s, see *Hastings et al. 1955*. Further, in many cases, n-vector representation is preferable *Gade 2010*, and they can be though of as just a different range reconstruction. Most iterative and closed form methods are straight-forward to convert. However, most polynomial methods are not, in a sensible way. Here matched inverse trigonometric function approximations are provided and dedicated (minimax) approximations for the n-vector representation.

Altogether, the mentioned (novel) components make polynomial approximations competitive again. Further, the computer development have probably contributed here too. Modern super-scalar vector CPUs are very good at evaluating polynomials, giving polynomial methods and edge over iterative and closed-form methods.

Note that iterative methods appear to have been around for a long time as well. The classical method by Hirvonen was first published in *Hirvonen 1959*[1]. *Morrison and Pines 1961* states *"Various procedures for obtaining a solution of these equations by iteration techniques exist."* without any further references. In turn, (published) exact solutions have been around since at least *Ecker 1967; Sugai 1967* with more following soon after *Tomelleri 1970; Paul 1973; Benning 1974; Hedgley 1976*. (Also *Ecker 1967* states that the transformation is normally carried out by iterative methods.) However, *Berger and Ricupito 1960* refers to solutions by *"Lagrange multiplier"* and *"high-degree algebraic equation"*. Further, *Vincenty 1985* claims the earliest closed form solution can be found in *Dörrie 1948* but, as pointed out by *Bajorek et al. 2014*, the latitude equation can be found e.g. on p49 in the book *Analytical Conics Sommerville 1924*. Finally, methods for solving quartic equations are known since Ferrari's 1545 solution, so exact solutions have probably been applied before Ecker's and Sugai's work.

3. Reductions, expansions and reconstructions

The multivariate and essentially unbounded nature of the coordinate transformation makes polynomial approximation techniques not directly applicable. The unboundedness is handled by the *range reduction* comprised of the ECEF to geocentric coordinates transformations

$$
(1) \qquad
\begin{aligned}
\phi_c &= \sin^{-1}(z/p) \\
\lambda_c &= \mathrm{atan2}(y, x) \\
h_c &= p - h_0
\end{aligned}
\qquad \text{and} \qquad
\bar{n}_c =
\begin{bmatrix} x/p \\ y/p \\ z/p \end{bmatrix}
=
\begin{bmatrix} r \\ s \\ t \end{bmatrix}
$$

where $p = \sqrt{x^2 + y^2 + z^2}$ and where ϕ_c, λ_c, h_c, h_0 and $\bar{n}_c$ are the geocentric latitude, longitude, altitude, reference radius and n-vector, respectively. Note that

$$
(2) \qquad
\bar{n} =
\begin{bmatrix} \cos(\phi)\cos(\lambda) \\ \cos(\phi)\sin(\lambda) \\ \sin(\phi) \end{bmatrix}
\quad \text{and} \quad
\bar{n}_c =
\begin{bmatrix} \cos(\phi_c)\cos(\lambda_c) \\ \cos(\phi_c)\sin(\lambda_c) \\ \sin(\phi_c) \end{bmatrix}
$$

and that $\lambda_c = \lambda$. Also note, later on, h_0 will be taken to be 0 but h_c and p are still kept separate since a non-zero h_0 could be used, or even some other expression for h_c. Clearly, ϕ_c, λ_c, r, s and t are bounded and h_c is bounded in the sense that an

---

[1] I have not yet managed to access the frequently cited 1958 publication by K. Rinner, or found any description of its results. Hence, it is not cited just yet.

interval of interest can typically be set. In turn, the multivariate nature is handled by the following key *series expansions* derived in Appendix A

(3)
$$\phi = \phi_c + t\sqrt{1-t^2}\omega(h_c, t^2) \qquad \sin(\phi) = \sin(\phi_c)\eta(t^2, \omega(h_c, t^2))$$
$$h = \mu(h_c, t^2) \qquad\qquad\qquad \cos(\phi) = \cos(\phi_c)\rho(t^2, \omega(h_c, t^2))$$

where, with the customary (abuse of) notation $\sum_{n=0}^{\infty}(\cdot)$ meaning $\lim_{N\to\infty}\sum_{n=0}^{N}(\cdot)$ and $\sum'$ meaning that the zeroth term is to be halved,

$$\omega(u, v) = \sum_{n=1}^{\infty}\sum_{k=0}^{n-1}(-1)^k\binom{2n}{2k+1}v^k(1-v)^{n-k-1}b_n(u)$$

$$\mu(u, v) = u + \sum_{n=0}^{\infty}{}'\sum_{k=0}^{n}(-1)^k\binom{2n}{2k}v^k(1-v)^{n-k}c_n(u)$$

$$\eta(v, w) = \sigma(\delta(v, w)) + (1-v)\tau(w, \delta(v, w))$$

$$\rho(v, w) = \sigma(\delta(v, w)) - v\tau(w, \delta(v, w))$$

where $b_n(\cdot)$ and $c_n(\cdot)$ are altitude dependent Fourier coefficients, encapsulating the *reference ellipsoid* properties, and

$$\delta(v, w) = v(1-v)w^2$$

$$\sigma(\delta) = \sum_{l\in\mathbb{N}_e}(-1)^{l/2}\frac{1}{l!}\delta^{l/2} \quad\text{and}\quad \tau(w, \delta) = w\sum_{l\in\mathbb{N}_o}(-1)^{(l-1)/2}\frac{1}{l!}\delta^{(l-1)/2}$$

where $\mathbb{N}_e$ and $\mathbb{N}_o$ are the sets of all positive even and odd natural numbers. Note, $\delta(t^2, \omega(h_c, t^2)) = (\phi - \phi_c)^2$, i.e. $\sigma(\delta)$ and $\tau(w, \delta)$ are polynomials in $(\phi - \phi_c)^2$. Further, note, the only assumption on ϕ and h in the derivation is that they are rotation symmetric with respect to the z-axis and that they are reflection anti-symmetric and symmetric, respectively, with respect to the xy-plane, i.e. the expressions are valid for any such quantities. The quantity specific attributes are carried by $b_n(\cdot)$ and $c_n(\cdot)$.

For h no *range reconstruction* is required whilst, from (2)-(3), it follows for n as

(4)
$$\bar{n} \approx \begin{bmatrix} r\,\rho(t^2, \omega,(h_c, t^2)) \\ s\,\rho(t^2, \omega,(h_c, t^2)) \\ t\,\eta(t^2, \omega,(h_c, t^2)) \end{bmatrix}$$

and for ϕ there are six reconstruction alternatives

(5)
$$\phi = \sin^{-1}\left(t\,\eta(t^2, \omega(h_c, t^2))\right) \qquad \phi = \text{sgn}(z)\cos^{-1}(q/p) + t\sqrt{1-t^2}\omega(h_c, t^2)$$

$$\phi = \sin^{-1}(t) + t\sqrt{1-t^2}\omega(h_c, t^2) \qquad \phi = \tan^{-1}(z/q) + t\sqrt{1-t^2}\omega(h_c, t^2)$$

$$\phi = \text{sgn}(z)\cos^{-1}\left(q/p\,\rho(t^2, \omega(h_c, t^2))\right) \quad \phi = \tan^{-1}\left(\frac{z\,\eta(t^2, \omega(h_c, t^2))}{q\rho(t^2, \omega(h_c, t^2))}\right)$$

where $q = \sqrt{x^2 + y^2}$. $\sin^{-1}$ is the least expensive to approximate but is ill-conditioned around the poles (the derivative goes to infinity) and using it anywhere near the poles requires a square root argument reduction. $\cos^{-1}$ requires a square root and a divide and is similarly ill-conditioned around the equator. $\tan^{-1}$ is well conditioned for all ϕ_c but requires a square root, a divide and some more arithmetic operations compared to $\sin^{-1}$ and $\cos^{-1}$. Similarly, the additive correction is ill-conditioned around the poles (the derivative of $t\sqrt{1-t^2}$ goes to infinity) whereas

the multiplicative correction is well conditioned for all ϕ_c. See Appendix B for some figures of what this ill-conditioning means.

As will be shown, for the least accurate approximations, $\sin^{-1}$-expressions are suitably used. Combining the $\sin^{-1}$ and $\cos^{-1}$ expressions for values around the poles gives potentially good performance but is a hard combination to tune, among other things to avoid discontinuous ϕ errors, and gives undesirable conditional code, and is not further investigated here. See Section 9 for some more discussion on it. For more accurate approximations, the $\tan^{-1}$ expressions are suitably used.

4. Partial polynomial approximations

The problem transformation of the previous sections reduces the transformation approximation problem to that of $\omega(u,v)$, $\mu(u,v)$, $\sigma(\delta)$, $\tau(w,\delta)$, $\sin^{-1}$, $\tan^{-1}$ and atan2. Naturally, minimax approximation are sought. The challenge is the two dimensional nature of $\omega(u,v)$ and $\mu(u,v)$. Fortunately, $\mu(u,v)$, being a Fourier cosine series, is a Chebyshev series with respect to v and truncated Chebyshev series give close to minimax approximations *Boyd 2001*. Similarly, truncation of $\omega(u,v)$ gives a close to minimax optimal approximation with respect to the weighting $v\sqrt{1-v^2}$. In contrast, for $b_n(h_c)$, $c_n(h_c)$ and $\sigma(\delta)$ and $\tau(w,\delta)$, explicit minimax approximations are used. Let

$$\{b_{n,m}^{(M)} : m \in [0,M]\} = \underset{\{b_m : m \in [0,M]\}}{\arg\min} \; \underset{h_c \in [h_{c\min}, h_{c\max}]}{\max} \left| b_n(h_c) - \sum_{m=0}^{M} b_m h_c^m \right|$$

$$\{c_{n,m}^{(M)} : m \in [0,M]\} = \underset{\{c_m : m \in [0,M]\}}{\arg\min} \; \underset{h_c \in [h_{c\min}, h_{c\max}]}{\max} \left| c_n(h_c) - \sum_{m=0}^{M} c_m h_c^m \right|$$

$$\{\varsigma_l^{(L)} : l \in [0, \lfloor L/2 \rfloor]\} = \underset{\{\varsigma_l : l \in [0, \lfloor L/2 \rfloor]\}}{\arg\min} \; \underset{\delta \in [0, \delta_{\max}]}{\max} \left| \sigma(\delta) - \sum_{l=0}^{\lfloor L/2 \rfloor} \varsigma_l \delta^l \right|$$

$$\{\vartheta_l^{(L)} : l \in [0, \lfloor (L-1)/2 \rfloor]\} = \underset{\{\vartheta_l : l \in [0, \lfloor (L-1)/2 \rfloor]\}}{\arg\min} \; \underset{\delta \in [0, \delta_{\max}]}{\max} \left| \tau(1,\delta) - \sum_{l=0}^{\lfloor (L-1)/2 \rfloor} \vartheta_l \delta^l \right|$$

where $b_{n,m}^{(M)}$ and $c_{n,m}^{(M)}$ are the mth coefficients of the minimax approximation of degree M with respect to h_c of the nth Fourier coefficients. Similarly, $\varsigma_l^{(L)}$ and $\vartheta_l^{(L)}$ are the lth coefficients of the minimax approximation of degree $\lfloor L/2 \rfloor$ and $\lfloor (L-1)/2 \rfloor$, respectively, i.e. a total degree of the multiplicative corrections of L. The ranges $[h_{c\min}, h_{c\max}]$ and $[0, \delta_{\max}]$ are the ranges over which the polynomial approximations are minimax optimal. See Section 6 for a discussions on $[h_{c\min}, h_{c\max}]$. In turn, $\delta_{\max}$ is defined by $[h_{c\min}, h_{c\max}]$ via

$$\delta_{\max} = \underset{\substack{h_c \in [h_{c\min}, h_{c\max}] \\ \phi_c \in [-\pi/2, \pi/2]}}{\max} \delta(\sin^2(\phi_c), \omega(h_c, \sin^2(\phi_c)))$$

$$= \underset{\substack{h_c \in [h_{c\min}, h_{c\max}] \\ \phi_c \in [0, \pi/2]}}{\max} (\phi - \phi_c)^2$$

Altogether, this gives the (essentially) minimax power series approximations

(6)
$$\begin{aligned} \omega(u,v) &\approx \omega_{N,M}(u,v) & \sigma(\delta) &\approx \sigma_L(\delta) \\ \mu(u,v) &\approx \mu_{N,M}(u,v) & \tau(w,\delta) &\approx \tau_L(w,\delta) \end{aligned}$$

where

$$\omega_{N,M}(u,v) = \sum_{n=1}^{N} \sum_{k=0}^{n-1} (-1)^k \binom{2n}{2k+1} v^k (1-v)^{n-k-1} \sum_{m=0}^{M} b_{n,m}^{(N)} u^m$$

$$\mu_{N,M}(u,v) = u + \sum_{n=0}^{N}{}' \sum_{k=0}^{n} (-1)^k \binom{2n}{2k} v^k (1-v)^{n-k} \sum_{m=0}^{M} c_{n,m}^{(M)} u^m$$

$$\sigma_L(\delta) = \sum_{l=0}^{\lfloor L/2 \rfloor} \varsigma_l^{(L)} \delta^l \quad \text{and} \quad \tau_L(w,\delta) = w \sum_{l=0}^{\lfloor (L-1)/2 \rfloor} \vartheta_l^{(L)} \delta^l$$

Minimax approximations are also naturally used for $\sin^{-1}$, $\tan^{-1}$ and atan2; math library functions are typically minimax approximations. Many different approximations are conceivable. *The focus here is not these approximations* for which a vast literature and tool sets exist, see e.g. *Muller 2006; Muller 2020; Darulova and Volkova 2019; Brunie et al. 2015*. However, to exemplify the performance and to make this work self-contained, basic approximations are used based on the sub-range ($[0,1]$ and $[-1,1]$) approximations

$$\{\alpha_i^{(I)} : i \in [0,I]\} = \underset{\{\alpha_i : i \in [0,I]\}}{\arg\min} \max_{x \in [0,1]} \left| \sin^{-1}(x) - \tfrac{\pi}{2} + \sqrt{1-x} \sum_{i=0}^{I} \alpha_i x^i \right|$$

$$\{\beta_j^{(J)} : j \in [0,J]\} = \underset{\{\beta_j : j \in [0,J]\}}{\arg\min} \max_{x \in [-1,1]} \left| \tan^{-1}(x) - \sum_{j=0}^{J} \beta_j x^{2j+1} \right|$$

and the resulting polynomials

$$\chi_I'(x) = \sum_{i=1}^{I} \alpha_i^{(I)} x^i \quad \text{and} \quad \xi_J'(x) = \sum_{j=0}^{J} \beta_j^{(J)} x^{2j+1}$$

These approximations are mapped to the full ranges by the following conditional-free bit-twiddling transformations

$$\sin^{-1}(x) \approx \chi_I(x) = \texttt{copysign}\left(\tfrac{\pi}{2} - \sqrt{1-|x|}\chi_I'(|x|), x\right)$$

(7) $$\tan^{-1}(y,x) \approx \psi_I(y,x) = \texttt{copysign}\left(\tfrac{\pi}{4} + \xi_J'\left(\tfrac{|y|-x}{|y|+x}\right), y\right) \quad \forall \quad x \geq 0$$

$$\text{atan2}(y,x) \approx \xi_J(y,x) = \pi d(y,x) + \texttt{copysign}\left(\tfrac{\pi}{4} + \xi_J'\left(\tfrac{|y|-|x|}{|y|+|x|}\right), x \oplus y\right)$$

where $d(y,x) = (((x \wedge y) \ggg (\texttt{sizeof}(x) \cdot 8 - 2)) \wedge -2) \vee (x \gg (\texttt{sizeof}(x) \cdot 8 - 1))$, and -2 within it, are Two's complement integers of the size of x and y implicitly converted to real in the multiplication with π and where $\texttt{copysign}(\cdot, \cdot)$ and $\texttt{sizeof}(\cdot)$ have the obvious (C/C++) meanings. Further, all logical operators ($\oplus$ is xor) are bit-wise and $\ggg$ and $\gg$ are bit shift with and without sign extension, respectively. Note, $\psi_I(0,0)$ and $\xi_J(0,0)$ contain $0/0$. For ϕ and $\psi_I(y,x)$ this is acceptable since it corresponds to the middle of the earth for which ϕ is not defined. For λ and $\xi_J(0,0)$ this is acceptable since it corresponds to the poles for which λ is not defined. Note the two argument version of arctangent $\tan^{-1}(y,x)$. In contrast to atan2(y,x), the second argument is limited and the output is in the range $[-\pi/2, \pi/2]$. The fact that the $\tan^{-1}$ argument can be split in a dividend and a *positive* divisor is instead used to make the mapping from $[-1,1]$ conditional free at the cost of two extra

additions. Further, note that the bit manipulations of the real values, which are typically implementation defined for most programming languages, only rely on the real value representation having an initial leading sign bit, so it is most likely possible to implement on almost all platforms but may require some extra care.

5. Complete polynomial approximations

Combining (2), (3), (5), (6), (4) and (7) gives the four latitude approximations

$$(8) \qquad \phi \approx \chi_I(t) + t\sqrt{1-t^2}\,\omega_{N_\phi,M_\phi}(h_c,t^2)$$

$$(9) \qquad \phi \approx \psi_I(z,q) + t\sqrt{1-t^2}\,\omega_{N_\phi,M_\phi}(h_c,t^2)$$

$$(10) \qquad \phi \approx \chi_I(t\,\eta_{L_\phi}(t^2,\omega_{N_\phi,M_\phi}(h_c,t^2)))$$

$$(11) \qquad \phi \approx \psi_I\left(z\,\eta_{L_\phi}(t^2,\omega_{N_\phi,M_\phi}(h_c,t^2)), q\rho_{L_\phi}(t^2,\omega_{N_\phi,M_\phi}(h_c,t^2))\right)$$

and the longitude, n-vector and altitude approximations

$$(12) \qquad \lambda \approx \xi_J(y,x)$$

$$(13) \qquad \bar{n} \approx \begin{bmatrix} r\,\rho_{L_n}(t^2,\omega_{N_n,M_n}(h_c,t^2)) \\ s\,\rho_{L_n}(t^2,\omega_{N_n,M_n}(h_c,t^2)) \\ t\,\eta_{L_n}(t^2,\omega_{N_n,M_n}(h_c,t^2)) \end{bmatrix}$$

$$(14) \qquad h \approx \mu_{N_h,M_h}(h_c,t^2)$$

From these follow the four *lla* ($\{\phi,\lambda,h\}$) transformation approximations

$$(15) \qquad \begin{aligned} f_{\sin+,\{N_\phi,M_\phi,N_h,M_h,I,J\}}(\{x,y,z\}) &= \{(8),(12),(14)\} \\ f_{\tan+,\{N_\phi,M_\phi,N_h,M_h,I,J\}}(\{x,y,z\}) &= \{(9),(12),(14)\} \\ f_{\sin\times,\{L_\phi,N_\phi,M_\phi,N_h,M_h,I,J\}}(\{x,y,z\}) &= \{(10),(12),(14)\} \\ f_{\tan\times,\{L_\phi,N_\phi,M_\phi,N_h,M_h,I,J\}}(\{x,y,z\}) &= \{(11),(12),(14)\} \end{aligned}$$

and the *nva* ($\{\bar{n},h\}$) transformation approximation

$$(16) \qquad f_{\bar{n},\{L_n,N_n,M_n,N_h,M_h\}}(\{x,y,z\}) = \{(13),(14)\}$$

for finite index limits I, J, L_ϕ, L_n, N_ϕ, M_ϕ, N_n, M_n, N_h and M_h.

6. Implementation

Implementing (15) and (16) entail computation of the coefficients, suitable polynomial transformations and arithmetic sequences for the polynomials and auxiliary quantities. For an application, a specific approximation with specific index limits, giving the best performance for a given platform for the desirable accuracy or computational cost design constraints, also have to be selected, i.e. a benchmark as exemplified in the next section should be carried out. (Many application will probably get away with just selecting an approximation from Appendix G.)

Further, the reference radius h_0 and the range $[h_{c\min}, h_{c\max}]$ are parameters of the approximations. Given minimax approximations, h_0 is of less importance and can be chosen as $h_0 = 0$, which eliminates one addition for each transformation. (If other polynomial approximations, i.e. Taylor, Padé, etc., are used, a non-zero h_0 will be of importance.) $[h_{c\min}, h_{c\max}]$ should cover all h_c values of an application. For most applications, it is easier to set an altitude range $[h_{\min}, h_{\max}]$ which gives $[h_{c\min}, h_{c\max}] = [h_{\min} + b - h_0, h_{\max} + a - h_0]$, where a and b are the reference ellipsoid semi-major and semi-minor axes. Note, even a zero altitude range still

requires a geocentric altitude range of $a - b \approx 21385$m. For the benchmark, the limits $h_{\min} = -5000$m and $h_{\max} = 100\,000$m are primarily used but results for larger and smaller ranges are also provided in Appendix D.

The computations of the coefficients $\varsigma_l^{(L)}$, $\vartheta_l^{(L)}$, $\alpha_i^{(I)}$ and $\beta_i^{(J)}$ only depend on arithmetic and elementary functions. Hence, they were easily computed with the Remez exchange algorithm implementation of `Sollya` 8.0 *Chevillard et al. 2010*. In contrast, the computations of the coefficients $b_{n,m}^{(M)}$ and $c_{n,m}^{(M)}$ were surprisingly hard. They appear numerically ill-conditioned and include numerical solutions of integrals making corresponding proper interval arithmetic challenging to implement. Instead, they were computed with a straight-forward basic Remez exchange algorithm implementation. However, to ensure that the linear system of the algorithm iterations were non-singular for the higher polynomial degrees and higher order Fourier coefficients, it had to be implemented with arbitrary precision arithmetic. Consequently, the integrals of $b_n(h_c)$ and $c_n(h_c)$ had to be solved numerically with arbitrary precision. This in turn requires reference transformations implemented in arbitrary precision. For the arbitrary precision arithmetic, the GMP *Granlund and the GMP development team 2012* (linked against), the MPFR *Fousse et al. 2007* (basic arbitrary precision arithmetic) and the MPLAPACK *Nakata 2022* (overloaded operators and arbitrary precision linear algebra) libraries were used. For the reference transformation, the closed-form transformation by *Vermeille 2004* was used. For the integrals, the Composite Simpson's 1/3 rule was used with 128 sub-intervals. (In principle something more suitable such as Clenshaw-Curtis integration should be used but, in practice, the integrals are benign enough to use Simpson's.) All computations were done with 200 bits of precision. The Remez algorithm termination criteria was set to ratio of the maximum and minimum error being less than $1 + 10^{-5}$. This gave coefficient values with $\sim$20 decimal digits of precision, giving some more precision than the ≤ 17 digits of double precision to handle final polynomial coefficients computations of $\omega_{N,M}(u, v)$ and $\mu_{N,M}(u, v)$, which were done with GiNaC 1.8.7 *2023*.

Beyond the coefficients, the polynomial evaluation has many degrees of freedom and even if arithmetic trees of minimal size could be found, in practice, they will typically be suboptimal due to instruction parallelism of modern superscalar processors and, in general, a large number of permutations has to be benchmarked for each polynomial order to find the best evaluation, a daunting task. See *Ewart et al. 2020* for a glimpse of what throughout optimization entails. And even an optimal evaluation, put in the overall arithmetic sequence, may not be optimal anymore. That said, Estrin's schema has been used as a middle-of-the-road approach. Only marginal differences has been observed in comparison with other general evaluation schema such as direct evaluation or Horner-2. The power factors of the schema were constructed by starting from the smallest power and solving the minimal *change-making* problem with respect to the already computed powers.

With the polynomials at hand, a reasonable overall arithmetic tree and an overall arithmetic sequence (traversal of the overall arithmetic tree/graph) of the polynomials and the auxiliary quantities is straight-forward to find. Pseudo-code of the approximations, defining such sequences are found in Table 1. The approximations of Table 1, as well as the literature methods, have been implemented in C++, using IEEE-754 double precision. Polynomial coefficients were pre-computed and

other derived constants computed at compile time. The implementations were compiled with gcc 13.2 with `-O3 -march=native`. `-O3` enables auto-vectorization and `-march=native` enables AVX instructions for the benchmark platform, which is beneficial for the polynomial evaluations. Results without AVX instructions are also provided in Appendix D.

7. Benchmark

The performance of the coordinate transformation methods are quantified with pairs of computational cost and error measurements. The desirable way to measure error may vary significantly for different applications. Hence, the results of multiple error measures are presented. In contrast, for most applications, the most interesting measure of computational cost, and the only one presented, is latency.

Normally, measuring anything but mean latency for algorithms is difficult, especially for the current algorithms since the latencies are in many cases data dependent. Hence, the mean has to be with respect to data. To separate the algorithm from the system influence, the minimum mean latency of multiple tests is used. The latency results were obtained with Nanobench 4.3 *Leitner-Ankerl 2022* using the minimum of the mean latency per sample of sets of 1000 samples repeated 10 000 times. This gave stable results for all methods. For further details of the latency measurements, see Appendix F.

Error measurements were separately computed with $5 \cdot 10^8$ uniformly distributed ECEF samples (ignoring elliptical effects) $\{x_k^\circ, y_k^\circ, z_k^\circ\}$ and geodetic references $\{\phi_k, \lambda_k, h_k\}$ and $\bar{n}_k$ over the volume of the respective altitude ranges, see *Rosca 2010* for details. The surface area of the earth is $\sim 5 \cdot 10^8 \text{km}^2$ so it means one sample per km^2. Extra samples were added around the poles, where methods frequently have sharp error peaks. All error computations were done in the Intel 80-bit extended precision format (`long double` on Linux), ensuring that the limits of the IEEE-754 double precision can be observed. Let $f_{lla/nva}(x, y, z)$ denote the transformation to be evaluated and the corresponding *lla* and *nva* transformation samples

$$\{\tilde{\phi}_k, \tilde{\lambda}_k, \tilde{h}_k\} = f_{lla}(x_k^\circ, y_k^\circ, z_k^\circ) \quad \text{and} \quad \{\tilde{n}_k, \tilde{h}_k\} = f_{nva}(x_k^\circ, y_k^\circ, z_k^\circ)$$

respectively. Further, for the *nva*, latitude and longitude values are computed with

$$\tilde{\phi}_k = \text{atan2}(n_{kz}, \sqrt{n_{kx}^2 + n_{ky}^2})$$

$$\tilde{\lambda}_k = \text{atan2}(n_{ky}, n_{kx})$$

with extended precision, where $\tilde{n}_k = [n_{kx}; n_{ky}; n_{kz}]$. Let $e_\alpha(\phi_k, \tilde{\phi}_k, \lambda_k, \tilde{\lambda}_k, h_k, \tilde{h}_k)$ and $e_\alpha(\phi_k, \tilde{\phi}_k, \lambda_k, \tilde{\lambda}_k, h_k, \tilde{h}_k, \bar{n}_k, \tilde{n}_k)$ denote α error measures for *lla* and *nva* transformations, respectively. See Appendix C for the definitions of the errors measures. The accuracy of $f_{lla/nva}(x, y, z)$ is then quantified with the maximum error

$$\max_k(|e_\alpha(\phi_k, \tilde{\phi}_k, \lambda_k, \tilde{\lambda}_k, h_k, \tilde{h}_k)|)$$

$$\max_k(|e_\alpha(\phi_k, \tilde{\phi}_k, \lambda_k, \tilde{\lambda}_k, h_k, \tilde{h}_k, \bar{n}_k, \tilde{n}_k)|)$$

respectively. (However, with the uniform samples, any statistics of the errors could be computed.)

For the polynomial approximations, the number of possible index limit combinations are too great for them to be exhaustively benchmarked. Initial narrowing of

$f_{\sin+,\{N_\phi,M_\phi,N_h,M_h,I,J\}}(\{x,y,z\})$	$f_{\tan+,\{N_\phi,M_\phi,N_h,M_h,I,J\}}(\{x,y,z\})$
$\quad p = \sqrt{x^2 + y^2 + z^2}$	$\quad p = \sqrt{x^2 + y^2 + z^2}$
$\quad t = z/p$	$\quad q = \sqrt{x^2 + y^2}$
$\quad t^2 = tt$	$\quad t = z/p$
$\quad \phi = \chi_I(t) + t\sqrt{1-t^2}\,\omega_{N_\phi,M_\phi}(p,t^2)$	$\quad t^2 = tt$
$\quad \lambda = \xi_J(y,x)$	$\quad \phi = \psi_I(z,q) + t\sqrt{1-t^2}\,\omega_{N_\phi,M_\phi}(p,t^2)$
$\quad h = \mu_{N_h,M_h}(p,t^2)$	$\quad \lambda = \xi_J(y,x)$
$\quad \text{return } \{\phi,\lambda,h\}$	$\quad h = \mu_{N_h,M_h}(p,t^2)$
	$\quad \text{return } \{\phi,\lambda,h\}$
$f_{\sin\times,\{L_\phi,N_\phi,M_\phi,N_h,M_h,I,J\}}(\{x,y,z\})$	$f_{\tan\times,\{L_\phi,N_\phi,M_\phi,N_h,M_h,I,J\}}(\{x,y,z\})$
$\quad p = \sqrt{x^2 + y^2 + z^2}$	$\quad p = \sqrt{x^2 + y^2 + z^2}$
$\quad t = z/p$	$\quad q = \sqrt{x^2 + y^2}$
$\quad t^2 = tt$	$\quad t^2 = (z/p)^2$
$\quad \omega = \omega_{N_\phi,M_\phi}(p,t^2)$	$\quad \omega = \omega_{N_\phi,M_\phi}(p,t^2)$
$\quad \delta = t^2(1-t^2)w^2$	$\quad \delta = t^2(1-t^2)w^2$
$\quad \sigma = \sigma_{L_\phi}(\delta)$	$\quad \sigma = \sigma_{L_\phi}(\delta)$
$\quad \tau = \tau_{L_\phi}(\omega,\delta)$	$\quad \tau = \tau_{L_\phi}(\omega,\delta)$
$\quad \phi = \chi_I(t(\sigma + (1-t^2)\tau))$	$\quad \phi = \psi_I\big(z(\sigma + (1-t^2)\tau), q(\sigma - t^2\tau)\big)$
$\quad \lambda = \xi_J(y,x)$	$\quad \lambda = \xi_J(y,x)$
$\quad h = \mu_{N_h,M_h}(p,t^2)$	$\quad h = \mu_{N_h,M_h}(p,t^2)$
$\quad \text{return } \{\phi,\lambda,h\}$	$\quad \text{return } \{\phi,\lambda,h\}$
$f_{\bar{n},\{L_n,N_n,M_n,N_h,M_h\}}(\{x,y,z\})$	
$\quad p = \sqrt{x^2 + y^2 + z^2}$	
$\quad t = z/p$	
$\quad t^2 = tt$	
$\quad \omega = \omega_{N_n,M_n}(p,t^2)$	
$\quad \delta = t^2(1-t^2)w^2$	
$\quad \sigma = \sigma_{L_n}(\delta)$	
$\quad \tau = \tau_{L_n}(\omega,\delta)$	
$\quad \rho' = (\sigma - t^2\tau)/p$	
$\quad \bar{n} = \big[x\rho', y\rho', t(\sigma + (1-t^2)\tau)\big]$	
$\quad h = \mu_{N_h,M_h}(p,t^2)$	
$\quad \text{return } \{\bar{n},h\}$	

TABLE 1. Pseudo-code implementation for the five different ECEF ($\{x,y,z\}$) to geodetic ($\{\phi,\lambda,h\}$ or $\{\bar{n},h\}$) coordinate transformations. Equality sign imply assignment. Powers are assumed implemented inline unless available as a left hand side variable. Note that $h_0 = 0$ and has been eliminated. A selection of polynomials can be found in Appendix G.

index limits is discussed in Appendix B. This still gives a test set of ~ 3000 index limit combination. Therefore, only results for selected approximations are labeled. The *nva* approximations have distinct error levels corresponding to different N. Consequently, the selection process is rather straight-forward. In contrast, the *lla* approximations demonstrates an almost continuous range of errors. Consequently, a simple selection of *lla* approximations matching the selected *nva* approximations is used. The selected, in the charts labeled and in Appendix G provided (corresponding polynomials) approximations are:

$f_{\bar{n},\{0,0,0,0,0\}}$ The simplest possible *nva* approximation corresponding to a spherical earth. The maximum Euclidean, horizontal and altitude errors are $2.1 \cdot 10^4$m, $2.1 \cdot 10^4$m and $1.1 \cdot 10^4$m, respectively.

$f_{\bar{n},\{1,1,0,1,0\}}$ $N = 1$ approximation with the maximum Euclidean, horizontal and altitude errors 85m, 85m and 13m, respectively. Note that there is a significant n-vector magnitude error of $2.8 \cdot 10^{-6}$. This gives an equivalent gravity error which is order of magnitude the same as typical gravity anomalies.

$f_{\bar{n},\{2,2,1,2,0\}}$ $N = 2$ approximation with the maximum Euclidean, horizontal and altitude errors 0.44m, 0.44m and 0.10m, respectively. The magnitude error is $9.9 \cdot 10^{-12}$. Note that there are faster approximations with roughly the same Euclidean error but with a significant magnitude error. The selected approximation gives the lowest relative gravity error of $6.8 \cdot 10^{-8}$ for the range, well below typical gravity anomalies.

$f_{\bar{n},\{3,3,2,3,2\}}$ $N = 3$ approximation with the maximum Euclidean, horizontal and altitude errors $1.2 \cdot 10^{-3}$m, $1.2 \cdot 10^{-3}$ and $4.8 \cdot 10^{-4}$m, respectively. The magnitude error is $6.7 \cdot 10^{-13}$.

$f_{\bar{n},\{3,4,3,4,2\}}$ $N = 4$ approximation with the maximum Euclidean, horizontal and altitude errors $4.7 \cdot 10^{-6}$m, $4.7 \cdot 10^{-6}$m and $1.2 \cdot 10^{-6}$m, respectively. The magnitude error is again $6.7 \cdot 10^{-13}$.

$f_{\bar{n},\{4,5,4,5,3\}}$ $N = 5$ approximation with the maximum Euclidean, horizontal and altitude errors $2.1 \cdot 10^{-8}$m, $2.1 \cdot 10^{-8}$m and $4.1 \cdot 10^{-9}$m, respectively. The magnitude error is at the numerical limit at $2.9 \cdot 10^{-16}$. Note, $L = 3$ gives a marginally faster approximation with essentially the same Euclidean error but the magnitude error become significant giving worse g approximation. (However, as noted, such g errors are below typical gravity anomalies.)

$f_{\bar{n},\{4,6,4,5,3\}}$ $N = 6$ approximation with the maximum Euclidean, horizontal and altitude errors just above the numerical limits at $5.5 \cdot 10^{-9}$m, $5.3 \cdot 10^{-8}$m and $4.1 \cdot 10^{-9}$m, respectively. The magnitude error is at the numerical limit at $2.9 \cdot 10^{-16}$. Note that the altitude approximation only has $N = 5$.

$f_{\sin\times,\{0,0,0,0,0,2,3\}}$ The simplest possible *lla* approximation. The Euclidean, horizontal and altitude errors are $2.0 \cdot 10^4$m, $2.0 \cdot 10^4$m and $1.1 \cdot 10^4$m, respectively.

$f_{\sin+,\{1,0,1,0,4,5\}}$ $N = 1$ approximation with Euclidean, horizontal and altitude errors of 114m, 113m and 13m, respectively.

$f_{\sin+,\{2,1,2,0,7,8\}}$ $N = 2$ approximation with Euclidean, horizontal and altitude errors of 0.41m, 0.40m and 0.10m, respectively.

$f_{\tan+,\{3,2,3,1,12,12\}}$ $N = 3$ approximation with Euclidean, horizontal and altitude errors of $1.2 \cdot 10^{-3}$m, $1.2 \cdot 10^{-3}$m and $4.8 \cdot 10^{-4}$m, respectively.

$f_{\tan\times,\{3,4,3,4,2,14,14\}}$ $N = 4$ approximation with Euclidean, horizontal and altitude errors of $7.9 \cdot 10^{-6}$m, $7.9 \cdot 10^{-6}$m and $1.2 \cdot 10^{-6}$m, respectively.

$f_{\tan\times,\{4,5,4,5,3,17,17\}}$ $N = 5$ approximation with Euclidean, horizontal and altitude errors of $2.5 \cdot 10^{-8}$, $2.5 \cdot 10^{-8}$ and $4.1 \cdot 10^{-9}$, respectively.

$f_{\tan\times,\{4,6,4,5,3,18,18\}}$ $N = 6$ approximation with Euclidean, horizontal and altitude error of $8.2 \cdot 10^{-9}$, $7.7 \cdot 10^{-9}$ and $4.1 \cdot 10^{-9}$, respectively. Note that the altitude approximation only has $N = 5$.

The results of the literature methods, against which the approximations are benchmarked, are labeled with numbers. These numbers and the corresponding methods are listed in chronological order below, together with short comments about the implementation and the results. Note that *all iterative methods have been implemented without trigonometric function evaluations in the iteration loop!* Methods of which trigonometric functions within the iteration loop has not been avoidable, e.g. *Jones 2002*, simply have much longer latencies and have not been included in the benchmark.

0	Spherical earth approximation. Not including any elementary function approximations, i.e. direct implementation of (1). This is in many ways the fastest (and least accurate) conceivable approximation and a special case of the presented method.
1-6	Iterative method by *Hirvonen 1959* with increasing number of iterations. The results start with zero iterations, using only the suggested initialization. Note that the method is often referred to as Hirvonen and Mortiz's since it appear in a publications bearing both names *Hirvonen and Moritz 1963*. Further, it is also often referred to as Heiksanen and Mortiz's since it appears in their 1967 book *Heiskanen and Moritz 1967*. Similarly, the same methods is also referred to as Torge's, e.g. *Voll 1990*, since it appears in *Torge 1975*.
7	Series expansion method by *Morrison and Pines 1961*. All but the necessary arctan:s have been replaced with multi-angle formulas and small angle approximations. The altitude formula has been replaced by that of Bowring.
8	Coarse method by *Gersten 1961*.
9-11	Method by *Baird 1964*. It performs poorly around the poles and, therefore, the maximum errors levels out. Closer than $\sim$ 6cm from the poles, it returns NaN and this area has been replaced with a spherical approximation.
12	Method by *Paul 1973*. It performs poorly around the equator, hence, the poor performance.
13-14	Original method by *Bowring 1976* with one and two iterations.
15	Closed form method by *Heikkinen 1982*.
16-18	Method by *Bowring 1976* with refined altitude calculations from *Bowring 1985* and 1-3 iterations.
19	Method by *Ozone 1985*. Poor conditioning makes the method perform poorly around the poles, hence the poor results. Except for the poles, it achieves the numerical precision.
20-26	Iterative method by *Wei 1986* starting from zero iterations.
27-33	Second iterative method by *Wei 1986* starting from zero iterations.
34-37	Method by Goad (1987) retrieved from *Voll 1990* with increasing number of iterations starting from zero.
38	Closed formula method by *Borkowski 1987* excluding inside-evolute handling.
39	Closed formula method by *Zhu 1994*.
40-42	Iterative method by *Lin and Wang 1995* with increasing number of iterations. The results start with zero iterations, using only the suggested initialization.
43	Approximation method by *Olson 1996*. No n-vector method is implementable since the algorithm works directly on the latitude.
44	Single iteration Bowrings's method optimized by *Toms 1996*. The method is not suitable for n-vector implementation.
45-50	Iterative method by *Sjöberg 1999* with increasing number of iterations starting from zero. The suggested polar region iterations are not implemented but rather only the adapted altitude formula *Wahlberg 2009*.
51-56	Iterative method by *Sjöberg 1999* with altitude computations according to *Bowring 1985*.
57-62	Iterative method by *Fukushima 1999* with increasing number of iterations.
63	Sofair's revised method *Sofair 2000*. It does perform particularly poor at the poles but not particularly good anywhere.
64-67	Iterative altitude first method by *Pollard 2002* with increasing number of iterations. The results start with two iterations. Less iterations gives error outside the plots.

68-71	Iterative latitude first method by *Pollard 2002* with increasing number of iterations. The results start with zero iterations, using only the suggested initialization.
72-74	Method by *Wu et al. 2003* with 0-2 iterations. One square root is avoided by reformulating the inverse cotangent to an inverse tangent and for the n-vector version, the altitude and n-vector normalization is done jointly, avoiding an extra square root.
75	Closed formula method by *Vermeille 2004* with n-vector version by *Gade and Gade 2007*.
76	Iterative method by *Fukushima 2006*. Note, with more than one iteration it is possible to find points for which it diverges. It also been noted for high altitudes by Ward *Ward 2020* but it may also happen for low altitudes.
77	Close form method by *Sjöberg 2008*.
78-83	Iterative method *a.2* by *Feltens 2008* with increasing number of iterations starting from zero iterations.
84-89	Iterative method *b.1* by *Feltens 2008* with increasing number of iterations starting from zero iterations.
90-91	Method by *Shu and Li 2010*.
92	Closed formula method by *Vermeille 2011* excluding inside evolute handling.
93-95	Method I by *Ligas and Banasik 2011* with one to three iterations.
96-97	Method II by *Ligas and Banasik 2011* with one and two iterations.
98	Method by *Karney 2011* provided in `GeographicLib` but with special handling for non-WGS84 spheroids removed. Note, this is an adaptation of *Vermeille 2004*.
99	Closed formula method by *Osen 2017*.
100-102	Perturbation method by *Hmam 2018* with increasing (3rd, 4th and 5th) order of the approximation.
103,104	Method by *Sampson 1982* and modified version by Claessens. Implementations from *Claessens 2019*.
105,106	Method by *Uteshev and Goncharova 2018* and modified version by Claessens. Implementations from *Claessens 2019*.
107	Bowring's method modified by *Claessens 2019*.
108	Spherical method by *Claessens 2019*.
109-111	Method by Dave Knopp found in the Peridetic code base *Knopp 2021* with 1-3 iterations.

In Figure 1 to 3, the latency results versus the different error measures are shown for a nominal altitude range of $[-5000, 100\,000]$m. Additional results for smaller and larger altitude ranges as well as result without AVX instructions are provided in Appendix D.

8. BENCHMARK DISCUSSION

The most important aspect of the benchmark is naturally correctness. As discussed in Appendix F, there are many factors influencing the results which together warrant a level of doubt in any benchmark results of this kind. Therefore, to minimize this doubt, in Appendix E, the benchmark machinery is cross-validated by reproducing results published elsewhere. It also contains some discussions about other benchmarks found in the literature, specifically note *Ward 2020* and *Voll 1990*.

About the results, the first thing to note are the outer bounds. The apparent lower numerical limits of the Euclidean, horizontal, altitude, latitude, longitude errors are comparable to the numerical precision (ulp) of IEEE-754 double precision of $\text{ulp}_{64}(a) \approx 9.3 \cdot 10^{-10}$. A further detailed numerical analysis is beyond the scope of this work. The upper limits are comparable to the difference between the major and minor axes, $a - b \approx 2.14 \cdot 10^4$. The lowest latency measurements ~ 10 clock cycles can be expected from a square root and a handful of arithmetic operations
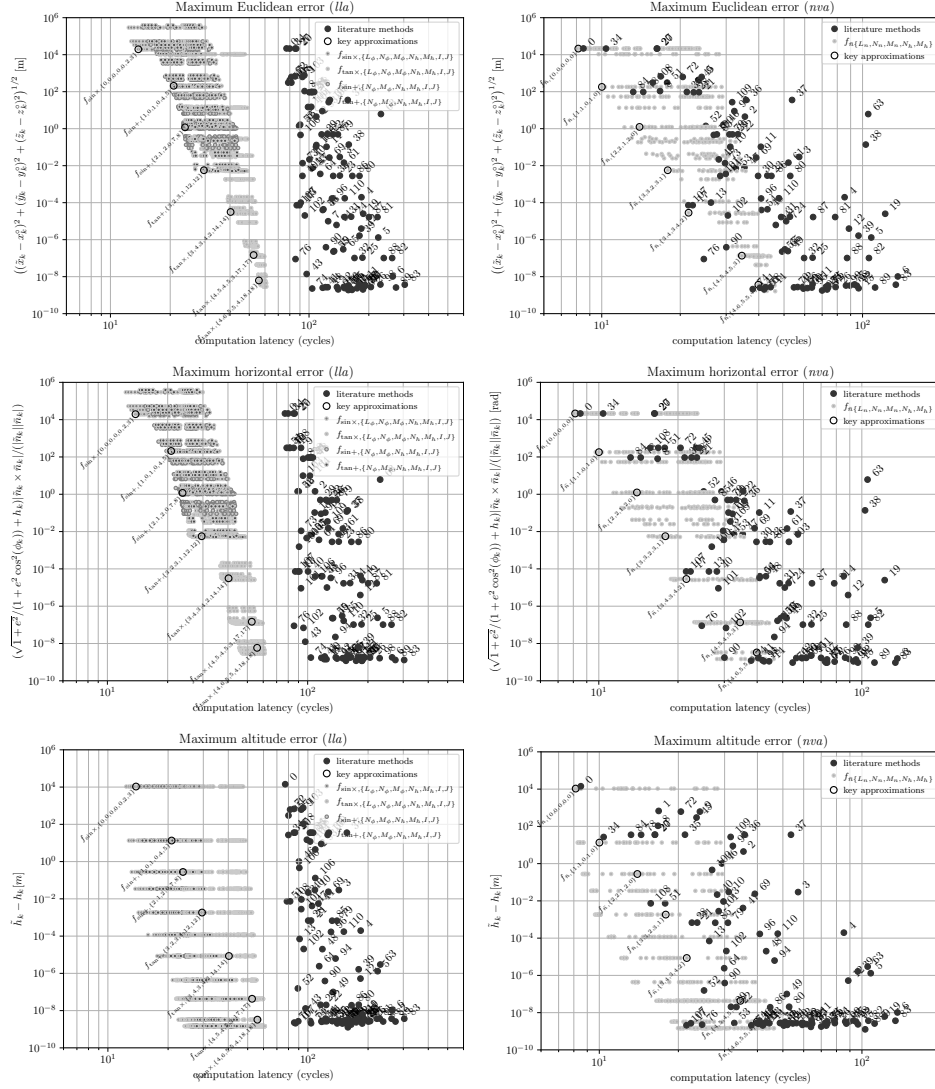
FIGURE 1. Total (Euclidean distance), horizontal (spherical and small angle approximation), and vertical (altitude) maximum absolute error over the volume of the altitude interval $[-5000, 100\,000]$. See Appendix C for detailed definitions. Grey points are the complete set of tested polynomial approximations. Circled and labeled points are approximation of particular interest. Black points are the indicated literature methods.
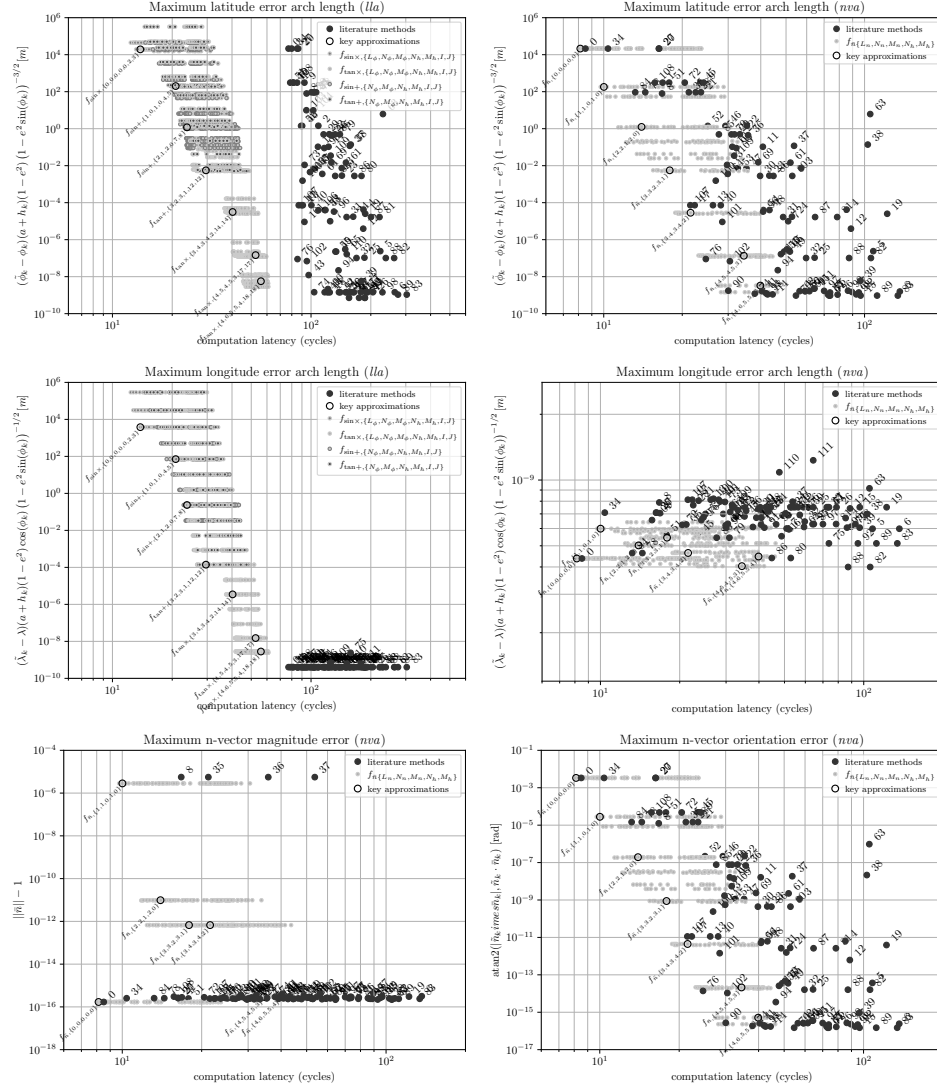
FIGURE 2. Latitude and longitude (arch length) and n-vector (magnitude and direction) maximum absolute error over the volume of the altitude interval [−5000, 100 000]. See Appendix C for detailed definitions. Grey points are the complete set of polynomial approximations. Black points are the indicated literature methods.
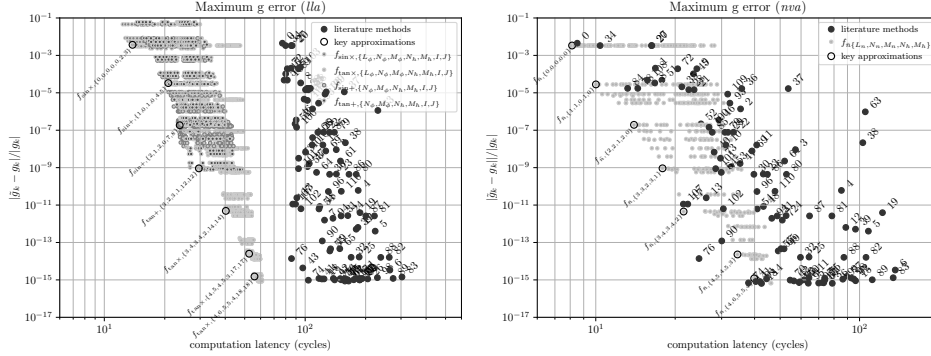
FIGURE 3. Fractional gravity (Euclidean distance) maximum absolute error over the volume of the altitude interval $[-5000, 100\,000]$. See Appendix C for detailed definitions. Grey points are the complete set polynomial approximations. Black points are the indicated literature methods. Clearly, even though the polynomial approximations introduces a magnitude error of the n-vector, they still improve on the achievable performance on the gravity computations.

of the spherical transformation approximation. The upper values of ~ 200 clock cycles can be expected from numerous square and cubic roots and a large number of arithmetic operations. Naturally, all these limits only changes marginally with varying altitude range. With a glance at the results for greater altitude ranges in Appendix D another outher bound may be observed. Simply, the presented methods becomes inefficient for altitude ranges beyond $\sim 10^6$. This sets a limit beyond which range splitting is required to use the presented methods. See discussion on improvements in the next section.

The second thing to note is that the *nva* latencies are roughly half that of the *lla* latencies, i.e. inverse trigonometric functions make up roughly half the cost of an *lla* method. The vast majority of *lla* methods contains the same inverse trigonometric functions, see *Olson 1996* for an exception, and, hence, the most relevant latencies are those for the *nva* methods. The differences between transformation methods are simply easier to observe when not diluted by common trigonometric components. However, not all methods can be converted to *nva* form and some applications requires *lla* representation so *lla* latencies are still relevant when comparing such methods, and for determining the computational cost for such applications. Note that latencies for trigonometric functions may vary significantly from implementation to implementation, e.g. see CORE-MATH benchmark The CORE-MATH project *2022*, requiring care when making comparison of absolute *lla* latency measurements from different sources.

From the *lla* results, it may appear that the presented approximations provide superior performance over the full accuracy range. However, the matched trigonometric approximations may be introduced to any method and, considering the *nva* result, a more balanced conclusion is rather that matched trigonometric approximations should be employed for any transformation method. Instead, the *nva* results, suggests that the presented approximations provide significantly improved performance down to $\sim 10^{-5}$m accuracy. Of course, the exact number depends on

the considered altitude range and may vary from platform to platform. For at hint on the variability of the results, see *Claessens 2019*.

Note, for the current approximations, the pattern that 1) the most preferable combination have identical N_ϕ and N_h values, 2) the Euclidean errors are normally almost identical to the horizontal errors and 3) the altitude errors are smaller than the horizontal errors, can be expected. From Fig. 4, for a given error, the altitude is less expensive to compute and, hence, for a given minimum maximum Euclidean error for a computational latency, the altitude error can be expected to be smaller. Further, for identical N_ϕ and N_h, the latitude and altitude errors are out-of-phase, which is preferable from an Euclidean error point of view. Combined with the fact that the altitude error can be expected to be smaller, the maximum Euclidean error can be expected to be dominated by the horizontal error.

Apart from the presented methods, below 10^{-5}, the following set of methods are within expected platform variability in terms of computational cost: *Bowring 1976* with modifications of *Bowring 1985*, *Olson 1996* (only *lla*), *Wu et al. 2003*, *Fukushima 2006* and *Shu and Li 2010*. Further, for very great altitude ranges *Hmam 2018* curiously appear to provide a relatively inexpensive and essentially altitude independent error. Beyond that, the benchmark results speaks for themselves. The horizontal, vertical, latitude and longitude errors can be viewed as basic error components and the Euclidean and g-errors can be viewed as examples of common application specific combined error measures. The n-vector errors are special errors primarily relevant for the presented method (containing explicit n-vector approximations).

9. Discussions

A set of fundamentally new ECEF to geodetic coordinate transformation approximations based on minimax polynomials have been presented. The benchmark results show that these approximations improves the achievable computational cost down to an accuracy of $\sim 10^{-5}$m. Corresponding improvements are also seen in other presented error measures and are large enough and shown in a convincingly large benchmark to be labeled *significant* despite natural uncertainties associated with the latency measurements. The improvements comes with the caveats that

- The approximations are valid over a preselected altitude range $[h_{\min}, h_{\max}]$ which has to be selected *before* the transformation are implemented. One cannot just iterate until convergence. Note that, a zero-range still imply an approximation range of $a - b \approx 21385$m.
- For the n-vector approximations, a magnitude error is also introduced.
- The performance of the methods is relatively improved by vector (AVX) instructions, especially for high order polynomials. Non-AVX results are provided in Appendix D.

On the other hand, for the vast majority of applications, the exemplified ranges will likely suffice and the *potential improvements* listing below contains several potential remedies for the problem. Moreover, even considering the magnitude errors, the approximation improves the achievable performance for e.g. gravity computations for which the n-vector magnitude enters directly. Finally, vector instructions have been prevalent in CPUs for more than a decade. Further, in addition to the improved performance, the approximations are attractive in that

- Explicit *nva* approximations are provided which is of particular importance for wide area physics simulations, e.g. flight and weather simulations, for which forces (gravity and drag) are computed many times but with moderate accuracy requirements.
- They resemble traditional polynomial approximations of elementary functions and related tools and techniques may be used to improve implementations and even to implement fixed-point versions, see e.g. *Mouilleron et al. 2014*.
- They are easy to specify and implement with straight-forward unbranching code only requiring regular arithmetic operations and the simplest elementary function, i.e. square-root, giving minimal dependencies on standard libraries. No special handling around the poles, the equator, etc. is required.
- The latitude, longitude, altitude and n-vector approximations are naturally separable making it possible to obtain only individual values at a lower computational cost.
- They are highly tunable in that a specific approximation may be selected to fulfill a computational cost or accuracy requirement. Especially, the horizontal and vertical accuracy can be set independently.
- Although only exemplified with WGS84 latitude and altitude, the method is extendable to a wider set of rotation symmetric and equatorial plan reflection symmetric and antisymmetric properties and the underlying series expansions may have a wider applicability within other geodesy problems enabling similar results to be obtained for these.
- The polynomial, separable and extendable nature of the components of the transformation approximation makes them amenable to vectorization (SIMD instructions) making them suitable for modern computational platforms.

In contrast, the greatest drawback and limitations of the approximations are that

- A large number of coefficients need to be precomputed to arrive at an actual approximation implementation, making the approximations somewhat hard to use out-of-the-box. Changing the preselected altitude range requires all coefficients to be recomputed.
- The convergence rate with respect to a greater number of coefficients indicates that the approximations becomes inefficient for accuracies beyond double precision, i.e. other methods have better error convergence rates.
- The results for great altitude ranges indicates that the approximations becomes inefficient for ranges beyond $\sim 10^6$m, i.e. handling such ranges requires range splitting.

However, coefficients covering most regular use-cases are provided in Appendix G and applications requiring more than double precision, i.e. subatomic accuracy, and ranges beyond $\sim 10^6$m, i.e. surface to orbital altitudes, are rare.

Clearly, the presented approximations sets a new standard for coarse (above $\sim 10^{-5}$m) and fast ECEF to geodetic coordinate transformations. Further, their polynomial nature opens up a new realm of further improvements. Specifically, note the following overall areas of potential improvement

- *Lookup tables* It is well known that many elementary functions are often implemented with a combination of minimax polynomials and coefficient

lookup tables rather than just a single polynomial. Diverging from clean arithmetic code, for many platforms, such strategies could probably be employed to further improve the approximation performance for the geodetic power series approximations. For the inverse trigonometric function approximations, this is definitely the case. Specifically, lookup tables with respect to p would be required to handle altitude ranges beyond $\sim 10^6$ but may be beneficial for much smaller altitude ranges as well.

- *Evaluation optimization* The expression trees of the individual (multivariat) polynomials have numerous degrees of freedom and the naive employed Estrin's schema are probably suboptimal, both in a number of operations sense and in a latency sense for a given platform. Hence, it may be improved upon both in a general sense, see e.g. *Kuipers et al. 2013*, and in a platform specific sense, see e.g. *Ewart et al. 2020*. The fact that the $\omega_{N,M}(\cdot,\cdot)$ and $\mu_{N,M}(\cdot,\cdot)$ polynomials are Bernstein polynomials with respect to $t^2 \in [0,1]$ could potentially be exploited, see e.g. *Chudy and Woźny 2021*. However, changing the individual evaluations schema may come in conflict with the following improvement option.

- *Cross polynomial evaluation optimization* The approximations are comprised of multiple polynomials with common factors and terms. This is only exploited through the polynomial arguments. However, more common components may be separated out and computed jointly in order to reduce the overall number of required arithmetic operations. For example, for specific N and M, joint evaluation schema for $\mu_{N,M}(u,v)$ and $\omega_{N,M}(u,v)$ with less arithmetic operations than the Horner scheme can be constructed. Further, as the results with and without AVX show, vectorization is important for performance. For platforms with vector operations, any evaluation schema has to take this into account and manual vectorization could potentially improve the latency. Furthermore, since the presented method can be extended to other geodetic quantities, vectorized method computing numerous such quantities at no extra cost may be constructed.

- *Alternative polynomial approximations* In general, regular minimax approximations provide good accuracy-to-computational-cost performance. However, weighted (relative) minimax, rational minimax, Padé or similar approximations may provide better performance. See *Turner 2009* and *Turner and Elgohary 2013* for examples. Other approximations may also give a different error growth relative some nominal h_0 which may be preferable for some applications. Further, it is also conceivable to parameterize the polynomials in $h_c{}^{-1}$ rather than h_c. This could provide better properties for great altitude ranges.

- *Full coefficient optimization* The polynomial approximations are split over inner and outer polynomials, with one assuming no errors in the other. Further, latitude, longitude and altitude errors are only connected via the index limits selection. This is clearly suboptimal and coefficients could potentially be adjusted to provide better overall approximations, i.e. higher-dimensional minimax approximations. Potentially, a low hanging fruit would be to replace the minimax optimization over h_c with the same over a first order altitude approximation.

- *Combined sin-cos approximations* Polynomial *lla* transformation approximations with accuracies below $\sim 10^{-4}$m combining $\sin^{-1}$ and $\cos^{-1}$ approximation for different t ranges with better performance than the presented approximations can easily be constructed. Note, in this case, neither the $\sin^{-1}$ nor the $\cos^{-1}$ approximations require a square root argument reduction. However, for a proper implementation, errors at the range extrema have to be matched to avoid error discontinuities. Further, approximation orders and ranges have to be optimized. This is, overall, a challenging but doable task.

- *Series expansions for coefficient calculations* The coefficients $b_n(u)$ and $c_n(u)$ are rather cumbersome to compute and, therefore, computing the corresponding minimax approximations is also cumbersome. The problem is that the integrals cannot be solved analytically and one has to resort to numerical integration. This could be circumvented by using series expansions for the differences. See for example *Long 1974*. The series sum could then be moved out of the integral and each term solved analytically resulting in a new series which would be much easier to implement and approximate with plain truncation. In turn, this would enable use of standard tools for computing the minimax approximations.

However, these are all very different technical areas from the work presented here and are left for future improvements.

10. Final recommendations

Before selecting a ECEF to geodetic coordinate transformation method, do review the actual application transformation requirements. Favor *nva* representation. Compared to *lla* representation and related methods, the computational cost is roughly half. If *lla* representation is required, make sure to use matched trigonometric function approximations. As for the actual transformation method: if the computational cost is important, the accuracy requirement is not below $\sim 10^{-5}m$ and the altitude range is below 10^6, do use the presented polynomial approximations. In contrast

- If computational cost is not a significant concern, use a closed form method like *Vermeille 2011* or *Karney 2011*. Then you do not have to consider number of iterations, matched trigonometric functions, accuracy, etc.

- If computational cost is important, the accuracy requirement is moderate (above $\sim 10^{-5}m$) but the altitude range cannot be bounded, instead consider methods by *Bowring 1976 + Bowring 1985* or *Shu and Li 2010* and make a look-up table in p for number of iterations until convergence. Be wary that the often suggested method by *Fukushima 2006* has numerical problems at very high altitudes. For astronomical altitude ranges, also consider *Hmam 2018*.

- If computational cost is important and the required accuracy is below $\sim 10^{-5}m$, also consider methods by *Bowring 1976 + Bowring 1985*, *Olson 1996*, *Wu et al. 2003*, *Fukushima 2006* and *Shu and Li 2010*.

Further, if you are implementing widely used library methods or computational resources are scarce and there is plenty of time and human resources, consider the areas of potential improvement of the previous section. Great altitude ranges can be handled and there is likely more performance to be found!

References

References are sorted in alphabetical order. References which have not been accessed are labeled accordingly and citations to one or more references citing and providing information about the inaccessible source are provided. To the extent possible, DOI:s or URL:s are provided.

Adams, O. S. (1921). *Latitude developments connected with geodesy and cartography*. Tech. rep. 67. United State Coast and Geodetic Survey. URL: `https://geodesy.noaa.gov/library/pdfs/Special_Publication_No_67.pdf`. (The linked report is the revised version from 1949. NOAA sort it under 1921 `https://geodesy.noaa.gov/library/`.)

Amiri-Simkooei, A. (Oct. 2002). "Comparison of different algorithms to transform geocentric to geodetic coordinates". In: *Survey Review* 36, pp. 627–633. DOI: `https://doi.org/10.1179/003962602791482966`.

Baird, R. W. (June 1964). *Cartesian Coordinate to Geodetic Coordinate Conversion*. White Sands Missile Range Data Reduction Directorate. (Not accessed, See *Voll 1990; Churchyard 1986*).

Bajorek, M., M. Kulczycki, and M. Ligas (Jan. 2014). "A comparison of iterative methods of the cubic rate convergence in the problem of transformation between Cartesian and geodetic coordinates". In: *Geomatics and Environmental Engineering* 8, p. 15. DOI: `https://doi.org/10.7494/geom.2014.8.2.15`.

Barbarella, M. and M. Gatti (Jan. 1993). "On the transformation from geocentric to ellipsoidal system". In: *Bollettino di Geodesia e Scienze Affini* 52, pp. 109–132. URL: `https://www.researchgate.net/publication/322884617_On_the_transformation_from_geocentric_to_ellipsoidal_system`. (In Italian).

Benning, W. (1974). "Der kürzeste Abstand eines in rechtwinkligen Koordinaten gegebenen Außenpunktes vom Ellipsoid". In: *Allgemeine Vermessungs-Nachrichten* 81.11, pp. 429–433. (Not accessed).

Berger, W. and J. Ricupito (1960). "Geodetic Latitude and Altitude of a Satelite". In: *ARS Journal* 30.9, pp. 901–902. DOI: `https://doi.org/10.2514/8.5262`.

Borkowski, K. (1987). "Transformation of Geocentric to Geodetic Coordinates Without Approximations". In: *Astrophysics and Space Science* 139, pp. 1–4. DOI: `https://doi.org/10.1007/BF00643807`.

Bowring, B. R. (1976). "Transformation from spatial to geographical coordinates". In: *Survey Review* 23, pp. 323–327. DOI: `https://doi.org/10.1179/sre.1976.23.181.323`.

Bowring, B. R. (1985). In: *Survey Review* 28.218, pp. 202–206. DOI: `https://doi.org/10.1179/sre.1985.28.218.202`. (Not accessed).

Boyd, J. P. (2001). *Chebyshev and Fourier Spectral Methods*. Second. Mineola, NY: Dover Publications.

Brunie, N. et al. (2015). "Code Generators for Mathematical Functions". In: *2015 IEEE 22nd Symposium on Computer Arithmetic*, pp. 66–73. DOI: `https://doi.org/10.1109/ARITH.2015.22`.

Burtch, R. C. (Apr. 2006). "A comparison of methods used in rectangular to geodetic coordinate transformations". In: *ACSM Annual Conference and Technology Exhibition*. Orlando, FL.

Chevillard, S., M. M. Joldeş, and C. Lauter (Sept. 2010). "Sollya: An Environment for the Development of Numerical Codes". In: *Mathematical Software - ICMS 2010*. Kobe, Japan, pp. 28–31. DOI: `https://doi.org/10.1007/978-3-642-15582-6_5`.

Chudy, F. and P. Woźny (2021). "Fast and accurate evaluation of dual Bernstein polynomials". In: *Numerical Algorithms* 87, pp. 1001–1015. DOI: `https://doi.org/10.1007/s11075-020-00996-5`.

Churchyard, J. N. (July 1986). "Comment on "A new algorithm for the computation of the geodetic coordinates as a function of earth-centered earth-fixed coordinates"". In: *Journal of Guidance, Control and Dynamics* 9.4, p. 511. DOI: https://doi.org/10.2514/3.20141.

Claessens, S. (Dec. 2007). *A comparison of techiques for the transformation from Cartesian to geodetic coordinates.* Presentation at IGNSS 2007 International Assembly, Sydney, Australia. URL: https://www.slideserve.com/macon/a-comparison-of-techniques-for-the-transformation-from-cartesian-to-geodetic-coordinates. (Presentation with benchmark summary not published elsewhere).

Claessens, S. (2019). "Efficient transformation from Cartesian to geodetic coordinates". In: *Computers & Geosciences* 133, p. 104307. DOI: https://doi.org/10.1016/j.cageo.2019.104307.

Darulova, E. and A. Volkova (2019). "Sound Approximation of Programs with Elementary Functions". In: *Computer Aided Verification.* Ed. by I. Dillig and S. Tasiran. Springer International Publishing, pp. 174–183. DOI: https://doi.org/10.1007/978-3-030-25543-5_11.

Deprit, A. and A. Deprit-Bartholome (Dec. 1975). "Conversion from geocentric to geodetic coordinates". In: *Celestial Mechanics* 12 (4), pp. 489–493. DOI: https://doi.org/10.1007/BF01595392.

Dörrie, H. (1948). *Kubische und biquadratische Gleichungen.* Berlin, Boston: Oldenbourg Wissenschaftsverlag. ISBN: 9783486775990. DOI: https://doi.org/10.1515/9783486775990.

Ecker, E. (1967). "Die Normalenfällung auf das Ellipsoid". In: *Österreichische Zeitschrift für Vermessungswesen* 55.3, pp. 82–85. URL: https://www.ovg.at/de/bibliothek/vgi-die-zeitschrift/files/pdf/4053.

Eissfeller, B. (1985). "A Taylor Series Expansion for the Transformation Problem of Cartesian Baseline Components into Ellipsoidal Coordinate Differences". In: *Schriftenreihe, Universitärer Studiengang Vermessungswesen, Universitaet der Bundeswehr München* 19, pp. 47–64. URL: https://www.unibw.de/geodaesie/bau-9-1-ingenieurgeodaesie/downloads/sonstige/heft-19.pdf.

Escapa, A. and T. Fukushima (July 2019). *Application of Lagrange Expansion Formula in Obtaining an Analytical Approximate Solution of Cartesian to Geodetic Transformation.* Presentation at: IUGG G05 Multi-Signal Positioning, Remote Sensing and Applications. DOI: https://doi.org/10.13140/RG.2.2.17838.25921.

Ewart, T. et al. (2020). "Polynomial Evaluation on Superscalar Architecture, Applied to the Elementary Function e^x". In: *ACM Transactions on Mathematical Software* 46.3. DOI: https://doi.org/10.1145/3408893.

Explanatory Supplement (1961). *Explanatory supplement to the astronomical ephemeris and the American ephemeris and nautical almanac.* London: H. M. Stationery Office. URL: https://archive.org/details/astronomicalalmanac1961. (Page 58).

Feltens, J. (Aug. 2008). "Vector methods to compute azimuth, elevation, ellipsoidal normal, and the Cartesian (X, Y, Z) to geodetic (ψ, λ, h) transformation". In: *Journal of Geodesy* 82, pp. 493–504. DOI: https://doi.org/10.1007/s00190-008-0246-5.

Fok, H. S. and H. B. Iz (Dec. 2003). "A Comparative Analysis of the Performance of Iterative and Non-iterative Solutions to the Cartesian to Geodetic Coordinate Transformation". In: *Journal of Geospatial Engineering* 5.2, pp. 61–74. URL: https://www.researchgate.net/publication/237622491_A_Comparative_Analysis_of_the_Performance_of_Iterative_and_Non-iterative_Solutions_to_the_Cartesian_to_Geodetic_Coordinate_Transformation.

Fousse, L. et al. (June 2007). "MPFR: A Multiple-Precision Binary Floating-Point Library with Correct Rounding". In: 33.2, pp. 13–28. DOI: https://doi.org/10.1145/1236463.1236468.

Fraser, W. (July 1965). "A Survey of Methods of Computing Minimax and Near-Minimax Polynomial Approximations for Functions of a Single Independent Variable". In: *Journal of ACM* 12.3, pp. 295–314. DOI: https://doi.org/10.1145/321281.321282.

Fukushima, T. (Dec. 1999). "Fast transform from geocentric to geodetic coordinates". In: *Journal of Geodesy* 73, pp. 603–610. DOI: https://doi.org/10.1007/s001900050271.

Fukushima, T. (Feb. 2006). "Transformation from Cartesian to Geodetic Coordinates Accelerated by Halley's Method". In: *Journal of Geodesy* 79, pp. 689–693. DOI: https://doi.org/10.1007/s00190-006-0023-2.

Gade, G. and K. Gade (2007). *n-vector – formulas with derivations*. Tech. rep. FFI/RAPPORT 2007/00633. Norwegian Defence Research Establishment (FFI). (Not accessed. See *Gade 2010*).

Gade, K. (2010). "A Non-singular Horizontal Position Representation". In: *The Journal of Navigation* 63.3, pp. 395–417. DOI: https://doi.org/10.1017/S0373463309990415.

Gersten, R. H. (1961). "Geodetic Sub-latitude and Altitude of a Space Vehicle". In: *The Journal of the Astronautical Sciences* 3.1, pp. 28–29. (Not accessed, See *Voll 1990*).

Getchell, B. C. (May 1972). "Geodetic Latitude and Altitude from Geocentric Coordinates". In: *Celestial Mechanics* 5.3, pp. 300–302. DOI: https://doi.org/10.1007/BF01228431.

GiNaC 1.8.7 (2023). https://www.ginac.de.

Granlund, T. and the GMP development team (2012). *GNU MP: The GNU Multiple Precision Arithmetic Library*. 5.0.5. http://gmplib.org/.

Gredan, G. P. (1999). "Transforming Cartesian coordinates X,Y,Z to Geographical coordinates ϕ, λ, h". In: *The Australian Surveyor* 44.1, pp. 55–63. DOI: https://doi.org/10.1080/00050351.1999.10558773.

Guo, J. C., X. X. Zhao, and Y. L. Wu (2014). "Transformation from Cartesian to geodetic coordinates using Lagrange inversion theorem". In: *Acta Geodaetica Et Cartographica Sinica* 43.10, pp. 998–1004. URL: http://xb.chinasmp.com/EN/Y2014/V43/I10/998. (In Chinese).

Hastings, C., J. T. Wayward, and J. P. Wong (1955). *Approximations for Digital Computers*. Princeton: Princeton University Press. DOI: https://doi.org/10.1515/9781400875597.

Hedgley David R., J. (Mar. 1976). *An exact transformation from geocentric to geodetic coordinates for nonzero altitudes*. Tech. rep. NASA Technical Report. URL: https://ntrs.nasa.gov/api/citations/19760012748/downloads/19760012748.pdf.

Heikkinen, M. (1982). "Geschlossene Formeln zur Berechnung räumlicher geodätischer Koordinaten aus rechtwinkligen Koordinaten". In: *Zeitschrift für Vermessungswesen* 107.5, pp. 207–211. (Not accessed).

Heiskanen, W. and H. Moritz (1967). *Physical Geodesy*. W.H. Freeman and Company. URL: https://archive.org/details/HeiskanenMoritz1967PhysicalGeodesy.

Helmert, F. R. (1880). *Die mathematischen und physikalischen theorieen der höheren geodäsie*. B. G. Teubner.

Hirvonen, R. A. (1959). *New theory of the gravimetric geodesy*. Tech. rep. 7. Ohio State University. Institute of Geodesy, Photogrammetry and Cartography. (Not accessed, See *Hirvonen and Moritz 1963*).

Hirvonen, R. A. (1960). *New theory of the gravimetric geodesy*. Tech. rep. Helsinki: Annales Academiae Scientarium Fennicae: Series A: III. Geologica - Geographica. (Not accessed, See *Hirvonen and Moritz 1963*).

Hirvonen, R. A. and H. Moritz (May 1963). *Practical Computation of Gravity at High Altitudes*. Tech. rep. 27. Institute of Geodesy, Photogrammetry and Cartagraphy. URL: https://archive.org/details/DTIC_AD0420541.

Hmam, H. (Feb. 2018). "Approximation solutions to the Cartesian to geodetic coordinate transformation problem". In: *Proceeding of the IGNSS Symposium*. Kensington, New South Wales, Australia.

ISO (Dec. 2011). *ISO/IEC 9899:2011 Information technology — Programming languages — C.* Geneva, Switzerland: International Organization for Standardization, 683 (est.) URL: `http://www.iso.org/iso/iso_catalogue/catalogue_tc/catalogue_detail.htm?csnumber=57853`.

Jones, G. C. (2002). "New solutions for the geodetic coordinate transformation". In: *Journal of Geodecy* 76, pp. 437–446. DOI: `https://doi.org/10.1007/s00190-002-0267-4`.

Karney, C. F. F. (2011). *Geodesics on an ellipsoid of revolution.* DOI: `https://doi.org/10.48550/arXiv.1102.1215`. arXiv: 1102.1215 [physics.geo-ph].

Karney, C. F. F. (June 2023). "On auxiliary latitudes". In: *Survey Review* 56.395, pp. 165–180. ISSN: 1752-2706. DOI: `http://dx.doi.org/10.1080/00396265.2023.2217604`.

Knopp, D. (2021). *Peridetic Transformations – Math Summary.* Tech. rep. Stellacore Corporation. URL: `https://github.com/Stellacore/peridetic`.

Kuipers, J. et al. (2013). "Improving multivariate Horner schemes with Monte Carlo tree search". In: *Computer Physics Communications* 184.11, pp. 2391–2395. ISSN: 0010-4655. DOI: `https://doi.org/10.1016/j.cpc.2013.05.008`.

Lapaine, M. (1991). "A New Direct Solution of the Transformation Problem of Cartesian into Ellipsoidal Coordinates". In: *Determination of the Geoid.* Ed. by R. H. Rapp and F. Sansò. New York, NY: Springer New York, pp. 395–404. ISBN: 978-1-4612-3104-2. DOI: `https://doi.org/10.1007/978-1-4612-3104-2_46`.

Leitner-Ankerl, M. (2022). *Nanobench.* `https://github.com/martinus/nanobench`.

Li, X. et al. (2022). "Simplified Expansions of Common Latitudes with Geodetic Latitude and Geocentric Latitude as Variables". In: *Applied Sciences* 12.15. DOI: `https://doi.org/10.3390/app12157818`.

Ligas, M. and P. Banasik (Jan. 2011). "Conversion between Cartesian and geodetic coordinates on a rotational ellipsoid by solving a system of nonlinear equations". In: *Geodesy and Cartography* 60, pp. 145–159. DOI: `https://doi.org/10.2478/v10277-012-0013-x`.

Lin, K.-C. and J. Wang (1995). "Transformation from geocentric to geodetic coordinates using Newton's iteration". In: *Belletin géodésique* 69, pp. 300–303. DOI: `https://doi.org/10.1007/BF00806742`.

Long, S. A. T. (Sept. 1974). *Derivation of transformation formulas between geodentric oand goedetic coordinates for nonzero altitudes.* Tech. rep. NASA. URL: `https://ntrs.nasa.gov/api/citations/19740021140/downloads/19740021140.pdf`.

Long, S. A. T. (1975). "General-altitude Transformations between Geocentric and Geodetic Coordinates". In: *Celestial Mechanics* 12.2, pp. 225–230. DOI: `https://doi.org/10.1007/BF01230214`.

Mikhailov, A. A. (May 1967). "The Reduction of Geocentric Latitude to Sea Level". In: *Soviet Astronomy* 10.6. URL: `https://articles.adsabs.harvard.edu/pdf/1967SvA...10.1052M`. Translated from Russian.

Morrison, J. and S. Pines (1961). "The reduction from geocentric coordinates". In: *The Astronomical Journal* 66.1, pp. 15–16. DOI: `https://doi.org/10.1086/108351`.

Mouilleron, C., A. Najahi, and G. Revy (2014). "Automated Synthesis of Target-Dependent Programs for Polynomial Evaluation in Fixed-Point Arithmetic". In: *2014 16th International Symposium on Symbolic and Numeric Algorithms for Scientific Computing,* pp. 141–148. DOI: `https://doi.org/10.1109/SYNASC.2014.27`.

Muller, J.-M. (2006). *Elementary functions - algorithms and implementation.* Birkhäuser Boston, MA. DOI: `https://doi.org/10.1007/b137928`.

Muller, J.-M. (2020). "Elementary Functions and Approximate Computing". In: *Proceedings of the IEEE* 108.12, pp. 2136–2149. DOI: `https://doi.org/10.1109/JPROC.2020.2991885`.

Nakata, M. (2022). *MPLAPACK version 2.0.1 user manual.* DOI: `https://doi.org/10.48550/arXiv.2109.13406`. arXiv: 2109.13406 [cs.MS].

Nautical Almanac (1931). *The Nautical Almanac And Astronomical Ephemeris For The Year 1931*. London: H.M. Stationery Office. URL: https://archive.org/embed/in.ernet.dli.2015.165859. (Page 718).

Newhall, X. X. (Mar. 1988). "Numerical representation of planetary ephemerides". In: *Celestial Mechanics* 45.1-3, pp. 305–310. DOI: https://doi.org/10.1007/BF01229014.

Nilsson, J.-O. (2024). *A comprehensive Cartesian to geodetic coordinate transformation reference listing*. DOI: https://doi.org/10.48550/arXiv.2405.05352. arXiv: 2405.05352 [physics.geo-ph].

Olson, D. . (1996). "Converting Earth-centered, Earth-fixed coordinates to geodetic coordinates". In: *IEEE Transactions on Aerospace and Electronic Systems* 32.1, pp. 473–476. DOI: http://doi.org/10.1109/7.481290.

Orihuela, S. (July 2013). *Funciones de Latitud*. Tech. rep. Universidad Nacional del Litoral. URL: https://www.academia.edu/7580468/Funciones_de_Latitud.

Osen, K. (2017). *Accurate Conversion of Earth-Fixed Earth-Centered Coordinates to Geodetic Coordinates*. Tech. rep. Norwegian University of Science and Technology. URL: https://hal.science/hal-01704943v2.

Ozone, M. I. (1985). "Non-Iterative Solution of the ϕ Equation". In: *Surveying and Mapping* 45.2, pp. 169–171. (Not accessed).

Paul, M. K. (June 1973). "A note on computation of Geodetic coordinates from geocentric (Cartesian) coordinates". In: *Bulletin Géodésique* 108 (1), pp. 135–139. DOI: https://doi.org/10.1007/BF02522075.

Pavlov, K. (1968). "Transformation de coordonnées rectangulaires spaciales X, Y, Z en coordonnées géographiques ϕ, λ, H pour les hauteurs inférieures a 10 km". In: *Schweizerische Zeitschrift für Vermessung, Photogrammetrie und Kulturtechnik* 66.12, pp. 381–388. DOI: https://doi.org/10.5169/seals-222321. (In French).

Pick, M. (1967). "Transformation of the spatial rectangular coordinates into the geodetic coordinates". In: *Bulletin Géodésique* 83, pp. 21–26. DOI: https://doi.org/10.1007/BF02526103.

Pollard, J. (Jan. 2002). "Iterative vector methods for computing geodetic latitude and height from rectangular coordinates". In: *Journal of Geodesy* 76, pp. 36–40. DOI: https://doi.org/10.1007/s001900100220.

Remez, E. Y. (1934). "Sur la détermination des polynômes d'approximation de degré donnée". In: *Comm. Soc. Math. Kharkov* 10 (41).

Rosca, D. (2010). "New uniform grids on the sphere". In: *Astronomy & Astrophysics* 520.A63. DOI: https://doi.org/10.1051/0004-6361/201015278.

Sampson, P. (Jan. 1982). "Fitting conic sections to "very scattered" data: An iterative refinement of the Bookstein algorithm". In: *Computer Graphics and Image Processing* 18, pp. 97–108. DOI: https://doi.org/10.1016/0146-664X(82)90101-0.

Shu, C. and F. Li (2010). "An iterative algorithm to compute geodetic coordinates". In: *Computers & Geosciences* 36.9, pp. 1145–1149. DOI: https://doi.org/10.1016/j.cageo.2010.02.004.

Sjöberg, L. E. (1999). "An efficient iterative solution to transform rectangular geocentric coordinates to geodetic coordinates". In: *Zeitschrift für Vermessungswesen* 124, pp. 295–297. (Not accessed).

Sjöberg, L. E. (2008). "A strict transformation from Cartesian to geodetic coordinates". In: *Survey Review* 40.308, pp. 156–163. DOI: https://doi.org/10.1179/003962608X290942. (Not accessed).

Sofair, I. (2000). "Improved Method for Calculating Exact Geodetic Latitude and Altitude Revisited". In: *Journal of Guidance, Control and Dynamics* 23.2, p. 369. DOI: https://doi.org/10.2514/2.4534.

Sommerville, D. M. Y. (1924). *Analytical Conics*. Bell's mathematical Series. London: G. Bell and Sons. URL: https://archive.org/details/dli.ernet.247333.

Sugai, I. (1967). "Note on Exact Geodetic Sub-Latitude and Geodetic Altitude of a Space Vehicle". In: *The Journal of the Astronautical Sciences* 14.3, pp. 134–137. (Not accessed. See *Lapaine 1991*).

Sünkel, H. (1976). "Ein nicht-iteratives Verfahren zur Transformation geodätischer Koordinaten". In: *Österreichische Zeitschrift für Vermessungswesen und Photogrammetrie* 64.1, pp. 29–33. URL: `https://www.ovg.at/de/bibliothek/vgi-die-zeitschrift/files/pdf/4216`.

The CORE-MATH project (2022). "`https://core-math.gitlabpages.inria.fr/`". Accessed: 2024-01-11.

Tomelleri, V. (1970). "L'asteriode tetracuspide retto ellittico bi-alettato e Ie coordiante alti-geografiche ellissoidi che di un punto assegnato". In: *Bollettino di geodesia e scienze affini* 29.1 and 2, 25-74 (1) and 137–166 (2). (Not accessed, See *Barbarella and Gatti 1993*, In Italian).

Toms, R. (Mar. 1996). "An Improved Algorithm for Geocentric to Geodetic Coordinate Conversion". In: *Proceedings on Standards for the Interoperability of Distributed Simulations*. Orlando, FL. URL: `https://www.osti.gov/servlets/purl/231228`.

Toms, R. M. (Mar. 1998). "New efficient procedures for geodetic coordinate transformations". In: *Proceedings on Standards for the Interoperability of Distributed Simulations*. Institute, for Simulation and Training, Orlando, FL, pp. 1024–1033. URL: `https://api.semanticscholar.org/CorpusID:115239162`.

Torge, W. (1975). *Geodäsie*. De Gruyter.

Torge, W. (2001). *Geodesy*. De Gruyter. DOI: `https://doi.org/10.1515/9783110879957.fm`.

Turner, J. D. (Feb. 2009). "A non-iterative and non-singular perturbation solution for transforming Cartesian to geodetic coordinates". In: *Journal of Geodesy* 83.2, pp. 139–145. DOI: `https://doi.org/10.1007/s00190-008-0247-4`.

Turner, J. D. and T. Elgohary (July 2013). "A Simple Perturbation Algorithm for Inverting the Cartesian to Geodetic Transformation". In: *Mathematical Problems in Engineering*. DOI: `https://doi.org/10.1155/2013/712729`.

Uteshev, A. Y. and M. V. Goncharova (2018). "Point-to-ellipse and point-to-ellipsoid distance equation analysis". In: *Journal of Computational and Applied Mathematics* 328, pp. 232–251. DOI: `https://doi.org/10.1016/j.cam.2017.07.021`.

Vermeille, H. (Sept. 2004). "Computing geodetic coordinates from geocentric coordinates". In: *Journal of Geodesy* 78 (1), pp. 94–95. DOI: `https://doi.org/10.1007/s00190-004-0375-4`.

Vermeille, H. (Feb. 2011). "An analytical method to transform geocentric into geodetic coordinates". In: *Journal of Geodesy* 85 (2), pp. 105–117. DOI: `https://doi.org/10.1007/s00190-010-0419-x`.

Vincenty, T. (1985). "Comment and Discussion, Re: Non-Iterative Solution of the ϕ Equation, by Mohammed Id Ozone". In: *Surveying and Mapping* 45.3, pp. 265–267. (Not accessed).

Voll, R. W. (May 1990). *Comparing The Accuracy and Efficiency of Algorithms For Converting Cartesian to Geodetic Coordinates*. Tech. rep. Faculty of the Virginia Polytechnic Institute and State University. URL: `http://hdl.handle.net/10919/41139`.

Wahlberg, T. (June 2009). "Undersökning av strikta och iterativa metoder för omvandling från kartesiska till geodetiska koordinater". MA thesis. KTH Royal Institute of Technology. URL: `http://kth.diva-portal.org/smash/get/diva2:1064960/FULLTEXT01.pdf`. (In Swedish).

Ward, S. (Feb. 2020). "Comparison of Earth-Centered, Earth-Fixed to Geodetic Coordinate Conversion Algorithms". In: *Simulation Innovation Workshop (SIW)*. Orlando, FL. URL: `https://github.com/planet36/ecef-geodetic/blob/main/docs/2020_SIW_16_modified.pdf`.

Wei, Z. (Aug. 1986). *Positioning with NAVSTAR, The Global Positioning System*. Tech. rep. 370. Department of Geodetic Science and Surveying, The Ohio State University. (Not accessed, See *Voll 1990*).

Wu, Y., P. Wang, and X. Hu (Nov. 2003). "Algorithm of Earth-centered Earth-fixed coordinates to geodetic coordinates". In: *IEEE Transactions on Aerospace and Electronic Systems* 39.4, pp. 1457–1461. DOI: `https://doi.org/10.1109/TAES.2003.1261144`.

Zanevičius, D. and F. Keršys (2010). "Technologies for calculating geodetic coordinates applying h-geometry functions". In: *Geodesy and Cartography* 36.4, pp. 160–163. DOI: `https://doi.org/10.3846/gc.2010.26`.

Zhu, J. (1994). "Conversion of Earth-centered Earth-fixed coordinates to geodetic coordinates". In: *IEEE Transactions on Aerospace and Electronic Systems* 30.3, pp. 957–961. DOI: `https://doi.org/10.1109/7.303772`.

Appendix A. Power series expansions

To handle the multivariate nature of the coordinate transformation, the approach is to express the difference between (1) and ϕ, h and $\bar{n}$ in Fourier (Chebyshev) series, with respect to ϕ_c and with h_c dependent coefficients. This separates the dependencies and enable truncation of the series with close to minimax properties. To start, relations between ϕ and ϕ_c and h and h_c are required. The actual analytical relations are of less importance and it is sufficient that they are numerically evaluable. Hence, let

$$\phi = f(x, y, z)$$
$$h = g(x, y, z)$$

be some reference ECEF-to-geodetic coordinate transformation of choice, e.g. see *Vermeille 2004*. (Note, the opaque nature of the reference means that the following derivation may be carried out for any $x = y = 0$ rotation symmetric and $z = 0$ plane reflection symmetric and anti-symmetric properties.) The geocentric to geodetic coordinate transformations follows as

$$\phi = f_c(\phi_c, h_c)$$
$$= f((h_c + h_0)\cos(\phi_c), 0, (h_c + h_0)\sin(\phi_c))$$
$$h = g_c(\phi_c, h_c)$$
$$= g((h_c + h_0)\cos(\phi_c), 0, (h_c + h_0)\sin(\phi_c))$$

$f_c(\cdot)$ and $g_c(\cdot)$ are naturally defined for $\phi_c \in [-\pi/2, \pi/2]$ and, hence, the differences between the geocentric and the geodetic coordinates, $f_c(\phi_c, h_c) - \phi_c = \phi - \phi_c$ and $g_c(\phi_c, h_c) - h_c = h - h_c$, are continuous and may be viewed as periodic with period π. Obviously, $\phi - \phi_c$ is antisymmetric and $h - h_c$ is symmetric around $\phi_c = 0$. Hence, they may be expressed as the Fourier sin and cos series

$$\phi - \phi_c = \sum_{n=1}^{\infty} b_n(h_c) \sin(2n\phi_c)$$

where

$$b_n(h_c) = \frac{2}{\pi} \int_{-\pi/2}^{\pi/2} (f_c(\phi_c, h_c) - \phi_c) \sin(2n\phi_c)\, \mathrm{d}\phi_c$$

and

$$h - h_c = \sideset{}{'}\sum_{n=0}^{\infty} c_n(h_c) \cos(2n\phi_c)$$

where

$$c_n(h_c) = \frac{2}{\pi} \int_{-\pi/2}^{\pi/2} (g_c(\phi_c, h_c) - h_c) \cos{(2n\phi_c)} \, \mathrm{d}\phi_c$$

Further, from the multi-angle formulas

$$\sin(2n\phi_c) = \sum_{k=0}^{n-1} (-1)^k \binom{2n}{2k+1} \sin^{2k+1}(\phi_c) \cos^{2n-2k-1}(\phi_c)$$

$$= \sin(\phi_c) \sqrt{1 - \sin^2(\phi_c)} \sum_{k=0}^{n-1} (-1)^k \binom{2n}{2k+1} \sin^{2k}(\phi_c)(1 - \sin^2(\phi_c))^{n-k}$$

$$\cos(2n\phi_c) = \sum_{k=0}^{n} (-1)^k \binom{2n}{2k} \sin^{2k}(\phi_c) \cos^{2n-2k}(\phi_c)$$

$$= \sum_{k=0}^{n} (-1)^k \binom{2n}{2k} \sin^{2k}(\phi_c)(1 - \sin^2(\phi_c))^{n-k}$$

It may not be obvious why a Fourier series expansion would be suitable but the fact that the differences are smooth and periodic gives a hint that a few series terms could be sufficient to make a good approximation of the differences. Further, from the multi-angle formulas, it can be seen that the Fourier series can be expressed as a power series in $\sin(\phi_c) = z/p$, which can easily be computed. Combining it all gives the expressions for the additive corrections to ϕ and h

(17)
$$\phi = \phi_c + \sin(\phi_c)\sqrt{1 - \sin^2(\phi_c)}\omega(h_c, \sin^2(\phi_c))$$
$$= \phi_c + t\sqrt{1 - t^2}\omega(h_c, t^2)$$
$$h = \mu(h_c, \sin^2(\phi_c))$$
$$= \mu(h_c, t^2)$$

where $\omega(\cdot, \cdot)$ and $\mu(\cdot, \cdot)$ are the power series

$$\omega(u, v) = \sum_{n=1}^{\infty} \sum_{k=0}^{n-1} (-1)^k \binom{2n}{2k+1} v^k (1-v)^{n-k-1} b_n(u)$$

$$\mu(u, v) = u + \sum_{n=0}^{\infty}{}' \sum_{k=0}^{n} (-1)^k \binom{2n}{2k} v^k (1-v)^{n-k} c_n(u)$$

Further, from (17) and the Taylor series of $\sin(\phi)$ and $\cos(\phi)$ around ϕ_c

$$\frac{\sin(\phi)}{\sin(\phi_c)} = \frac{\sin\left(\phi_c + \sin(\phi_c)\sqrt{1 - \sin^2(\phi_c)}\omega(h_c, \sin^2(\phi_c))\right)}{\sin(\phi_c)}$$

$$= \sum_{l=0}^{\infty} \left.\frac{\partial^l}{\partial \varphi^l}\frac{\sin(\varphi)}{l!}\right|_{\phi_c} \frac{\left(\sin(\phi_c)\sqrt{1 - \sin^2(\phi_c)}\omega(h_c, \sin^2(\phi_c))\right)^l}{\sin(\phi_c)}$$

$$= \sum_{l \in \mathbb{N}_e}(-1)^{l/2}\frac{1}{l!}\left(\sin(\phi_c)\sqrt{1 - \sin^2(\phi_c)}\omega(h_c, \sin^2(\phi_c))\right)^l$$

$$+ \sum_{l \in \mathbb{N}_o}(-1)^{(l-1)/2}\frac{1}{l!}\frac{\cos(\phi_c)}{\sin(\phi_c)}\left(\sin(\phi_c)\sqrt{1 - \sin^2(\phi_c)}\omega(h_c, \sin^2(\phi_c))\right)^l$$

$$= \sum_{l \in \mathbb{N}_e}(-1)^{l/2}\frac{1}{l!}(\sin^2(\phi_c))^{l/2}(1 - \sin^2(\phi_c))^{l/2}\omega(h_c, \sin^2(\phi_c))^l$$

$$+ \sum_{l \in \mathbb{N}_o}(-1)^{(l-1)/2}\frac{1}{l!}(\sin^2(\phi_c))^{(l-1)/2}(1 - \sin^2(\phi_c))^{(l+1)/2}\omega(h_c, \sin^2(\phi_c))^l$$

$$\frac{\cos(\phi)}{\cos(\phi_c)} = \frac{\cos\left(\phi_c + \sin(\phi_c)\sqrt{1 - \sin^2(\phi_c)}\omega(h_c, \sin^2(\phi_c))\right)}{\cos(\phi_c)}$$

$$= \sum_{l=0}^{\infty} \left.\frac{\partial^l}{\partial \varphi^l}\frac{\cos(\varphi)}{l!}\right|_{\phi_c} \frac{\left(\sin(\phi_c)\sqrt{1 - \sin^2(\phi_c)}\omega(h_c, \sin^2(\phi_c))\right)^l}{\cos(\phi_c)}$$

$$= \sum_{l \in \mathbb{N}_e}(-1)^{l/2}\frac{1}{l!}\left(\sin(\phi_c)\sqrt{1 - \sin^2(\phi_c)}\omega(h_c, \sin^2(\phi_c))\right)^l$$

$$+ \sum_{l \in \mathbb{N}_o}(-1)^{(l+1)/2}\frac{1}{l!}\frac{\sin(\phi_c)}{\cos(\phi_c)}\left(\sin(\phi_c)\sqrt{1 - \sin^2(\phi_c)}\omega(h_c, \sin^2(\phi_c))\right)^l$$

$$= \sum_{l \in \mathbb{N}_e}(-1)^{l/2}\frac{1}{l!}(\sin^2(\phi_c))^{l/2}(1 - \sin^2(\phi_c))^{l/2}\omega(h_c, \sin^2(\phi_c))^l$$

$$+ \sum_{l \in \mathbb{N}_o}(-1)^{(l+1)/2}\frac{1}{l!}(\sin^2(\phi_c))^{(l+1)/2}(1 - \sin^2(\phi_c))^{(l-1)/2}\omega(h_c, \sin^2(\phi_c))^l$$

where $\mathbb{N}_e$ and $\mathbb{N}_o$ are the sets of all positive even and odd natural numbers. Let

$$\delta(v, w) = v(1 - v)w^2$$

$$\sigma(\delta) = \sum_{l \in \mathbb{N}_e}(-1)^{l/2}\frac{1}{l!}\delta^{l/2} \quad \text{and} \quad \tau(w, \delta) = w\sum_{l \in \mathbb{N}_o}(-1)^{(l-1)/2}\frac{1}{l!}\delta^{(l-1)/2}$$

and

$$\eta(v, w) = \sigma(\delta(v, w)) + (1 - v)\tau(w, \delta(v, w))$$

$$\rho(v, w) = \sigma(\delta(v, w)) - v\tau(w, \delta(v, w))$$

Then, multiplicative sin and cos corrections follow as

$$\sin(\phi) = \sin(\phi_c)\eta(t^2, \omega(h_c, t^2))$$
$$\cos(\phi) = \cos(\phi_c)\rho(t^2, \omega(h_c, t^2))$$

APPENDIX B. REASONABLE INDEX LIMIT COMBINATIONS

The polynomial orders determines the absolute errors and computational costs. Hence, they will, to some extent, be application and platform specific and will ultimately have to be set by benchmarking different combinations, which is done in Section 7. Unfortunately, the combinations $\{I, J, L_\phi, N_\phi, M_\phi, N_h, M_h\} \in \mathbb{N}^7$ or $\{I, J, N_\phi, M_\phi, N_h, M_h\} \in \mathbb{N}^6$, for the *lla* approximations, and $\{L_n, N_n, M_n, N_h, M_h\} \in \mathbb{N}^5$, for the *nva* approximations, are too many to be tested exhaustively. Therefore, the combinations have to be narrowed down based on their relative errors which is here made based on the three assumptions

- Applications typically have a horizontal accuracy requirement rather than separate latitude and longitude accuracy requirements. Hence, $\{I, J, L_{\phi/n}, N_{\phi/n}, M_{\phi/n}\}$ are narrowed down jointly.
- Applications may have vastly different requirements on horizontal and vertical accuracy. Hence, $\{I, J, L_{\phi/n}, N_{\phi/n}, M_{\phi/n}\}$ and $\{N_h, M_h\}$ are narrowed down independently.
- A part from position error, L_n also affect n-vector magnitude errors, which are hard to compare and significant for $L_\phi \leq 3$. Hence, for $L_\phi \leq 3$ the limitations set by L_ϕ are ignored.

Starting from sufficiently high limits, attaining horizontal (latitude and longitude) and altitude errors at the numerical limits of the IEEE-754 double precision implementation, and lowering one limit at at a time gives the maximum error shown in Fig. 4. Let $E_K^{f_i}(\cdot)$ denote the values shown in Fig. 4 for the respective approximation f_i and index limit K. Start with complete sets of index limit value combinations $\{L, N, ...\}$. Split according to the assumptions. Let $E_{\max}^{f_i} = \max_K(\{E_K^{f_i}(X) : X \in \{L, N, ...\}\}$ be the maximum error for such a set. Then reject the combinations if either

- $K > K_{\min}$ and $E_K^{f_i}(K - 1) < E_{\max}^{f_i}$ and $E_K^{f_i}(K) < E_{\max}^{f_i}0.25$
- $K > K_{\min}$ and $E_K^{f_i}(K) < 0.95 E_K^{f_i}(K - 1)$

The first conditions handles the potential constructively or destructively inference between errors, meaning the combinations cannot be reduced to the index limits providing limiting errors closest to each other. The second condition handles increasing index limits not reducing the errors more. 0.25 and 0.95 are trade-offs between ensuring that all reasonable combinations are captured and limiting the total number of tested combination. 0.25 and 0.95 give ~ 3000 combinations to test for the benchmark.

APPENDIX C. ERROR DEFINITIONS

The errors used in the comparison of different approximations and literature methods are defined as follows. Throughout, the *Earth's prime-vertical radius of curvature* is $\tilde{N}_k = a^2(a^2 \cos^2(\tilde{\phi}_k) + b^2 \sin^2(\tilde{\phi}_k))^{-1/2}$ and *Earth's meridional radius of curvature* $\tilde{M}_k = (1 - e^2)/a^2 \tilde{N}_k^3$. Note, for $\{x, y, z\} = \{0, 0, 0\}$ only altitude error is well defined but this is not repeated for every measure.
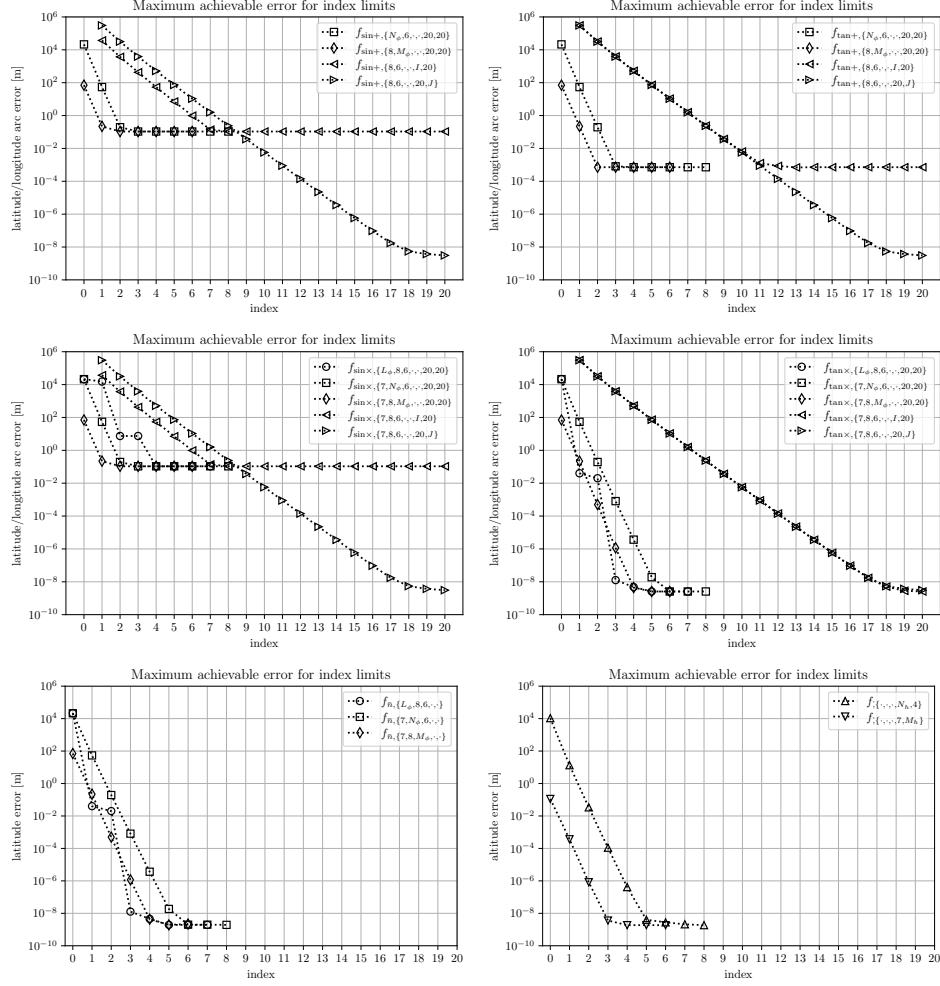
FIGURE 4. Maximum error (latitude arc error, longitude arc error and altitude error) of the labeled approximation and index limit set to the indicated value and the remaining index limits set to $I = 20$, $J = 20$, $L_{\phi/n} = 6$, $N_{\phi/h/n} = 8$, $M_{\phi/h/n} = 6$. This provides an approximate achievable lower maximum error limit given individual index limits. The leveling out of some of the curves above the numerical limit of 10^{-1} is caused by poor numerical conditioning and corresponding errors of $\sin^{-1}$, i.e. χ_I, and $t\sqrt{1-t^2}$ around the poles.

- Euclidean error in meter

$$e_{\leftrightarrow} = \sqrt{(\tilde{x}_k - x_k^\circ)^2 + (\tilde{y}_k - y_k^\circ)^2 + (\tilde{z}_k - z_k^\circ)^2}$$

where

$$\tilde{x}_k = \left(\tilde{N}_k + \tilde{h}_k\right)\cos(\tilde{\phi}_k)\cos(\tilde{\lambda}_k)$$

$$\tilde{y}_k = \left(\tilde{N}_k + \tilde{h}_k\right)\cos(\tilde{\phi}_k)\sin(\tilde{\lambda}_k)$$

$$\tilde{z}_k = \left(\tfrac{b^2}{a^2}\tilde{N}_k + \tilde{h}_k\right)\sin(\tilde{\phi}_k)$$

- Geodetic horizontal error in meter. Computing the error is equivalent to the *inverse geodetic problem*. However, since the errors (distances) can be assumed small, sufficient accuracy can be achieved with a local spherical approximation which can be further simplified

$$e_\frown = (\sqrt{1+e^2}/(1+e^2\cos^2(\phi_k)) + h_k)\,\mathrm{atan2}(|\tilde{n}_k \times \bar{n}_k|, \tilde{n}_k \cdot \bar{n}_k)$$

$$\approx (\sqrt{1+e^2}/(1+e^2\cos^2(\phi_k)) + h_k)|\tilde{n}_k \times \bar{n}_k|/(|\tilde{n}_k||\bar{n}_k|)$$

where $\sqrt{1+e^2}/(1+e^2\cos^2(\phi_k)) + h_k$ is the local spherical curvature radius and $e^2 = (1 - b^2/a^2)$ is the Earth's eccentricity.

- Latitude error arch length in meter. This in general requires a numerical solution of the *meridian arc* but for small error $\tilde{\phi}_k - \phi_k$, relative to the change in curvature of the earth, it can be approximated with

$$e_\phi = (\tilde{\phi}_k - \phi_k)(a + h_k)/a\tilde{M}_k$$

- Longitude error arch length in meter

$$e_\lambda = \begin{cases} \phi_k = \pi/2 & 0 \\ \text{otherwise} & (\tilde{\lambda}_k - \lambda_k)\cos(\phi_k)(a + h_k)/a\tilde{N}_k \end{cases}$$

Longitude is not defined for the polar axis and the errors there is always 0.

- Altitude error in meter

$$e_h = \tilde{h}_k - h_k$$

- Fractional gravity vector error based on Somigliana's (WGS84) gravity formula with second order free-air anomaly correction *Torge 2001*

$$g(\phi, h) = \gamma_a \frac{1 + \kappa_g \sin(\phi)}{(1 - e^2\sin(\phi))^{-1/2}}(1 - (\kappa_1 - \kappa_2\sin(\phi))h + \kappa_3 h^2)$$

where
  - $\kappa_g = \frac{b\gamma_b}{a\gamma_a} - 1$
  - $\gamma_a = 9.780\,326\,771\,5$ m/s^2 is the gravity at the equator
  - $\gamma_b = 9.832\,186\,368\,5$ m/s^2 is the gravity the poles
  - $\kappa_1 = 2(1 + f + m)/a = 3.157\,04 \cdot 10^{-7}$m^{-1}
  - $\kappa_2 = 4f/a = 2.102\,69 \cdot 10^{-9}$m^{-1}
  - $\kappa_3/a^2 = 7.374\,52 \cdot^{-14}$ m^{-1}

giving the error

$$e_g = ||g(\tilde{\phi}_k, \tilde{h}_k)\tilde{n}_k - g(\phi_k, h_k)\bar{n}_k||/|g(\phi_k, h_k)|$$

- N-vector magnitude error

$$e_{|n|} = 1 - ||\tilde{n}_k||$$

- N-vector orientation error in radians

$$e_{\arg(n)} = \text{atan2}(|\tilde{n}_k \times \bar{n}_k|, \tilde{n}_k \cdot \bar{n}_k)$$

This may be implemented as

$$e_{\arg(n)} = \sin^{-1}(|\tilde{n}_k \times \bar{n}_k|/|\tilde{n}_k|\bar{n}_k|)$$
$$\approx |\tilde{n}_k \times \bar{n}_k|/(|\tilde{n}_k||\bar{n}_k|)$$

for angles below $\pi/2$ and small angles, respectively.

Appendix D. More benchmark results

Additional results for smaller and larger altitude ranges as well as for methods compiled without AVX support are provided in Fig. 5 and Fig. 6, respectively.

Appendix E. Other benchmarks and benchmark cross-validation

The results can only partially be compared with other results found in the literature. Foremost, there are no other benchmarks considering *nva* performance. Further, the only extensive modern benchmark found in the literature is *Ward 2020*. There is also an early interesting benchmark *Voll 1990* but it is somewhat too old and has too poor code standard to be of interest for latency measurement comparison. Worth mentioning is also the solid but narrow benchmark *Bajorek et al. 2014*. Frequently cited is the benchmark *Gredan 1999* but it is too small to be of general interest. In addition, a few more benchmarks can be found *Amiri-Simkooei 2002* and *Fok and Iz 2003*. However, they are of such poor quality that they can largely be ignored. A small benchmark can also be found in *Wahlberg 2009* (Swedish) and a review of methods in *Burtch 2006*. Further, most articles presenting transformation methods comes with some benchmark but they are generally too small to draw far reaching conclusions.

Absolute timing results are scarce in the literature. A comparison of latency measurements of transformation methods overlapping with those of *Ward 2020* is provided in the first plot of Fig. 7, together with a least squares line fit. Performance variation figures presented in *Claessens 2019* indicate that differences of 5-10% can be expected even for identical implementations. Hence, the deviation from the linear fit can be expected. Further, the latencies was measured on an Intel Core i7 1185G7 (current) and on an Intel Core i9 13950HX (Ward). From CPU single core benchmark results, the difference can be expected to be +45% which is in line with 0.65 (+54%). Finally, the small constant part indicate that the measurement overhead is low. Altogether, this provides an additional confidence in the latency measurements. Some other timing results can also be found in the literature. In *Fukushima 2006*, latencies are provided for 8 methods but they are in the range $[500, 5000]$ and clearly too old to be comparable.

Maximum error results are more common and results from Ward *Ward 2020*, Claessens *Claessens 2019*, Ligas and Banasik *Ligas and Banasik 2011* and Lin and Wang *Lin and Wang 1995* are compared against error results produced by the current benchmark machinery in the second plot of Fig. 7. The results are a mix of Euclidean distance, latitude errors and altitude errors, all converted to distances in meter. Ideally all results should fall on the $y = x$ line included in the plot. Most results are spot on while some results deviate considerably. Specifically
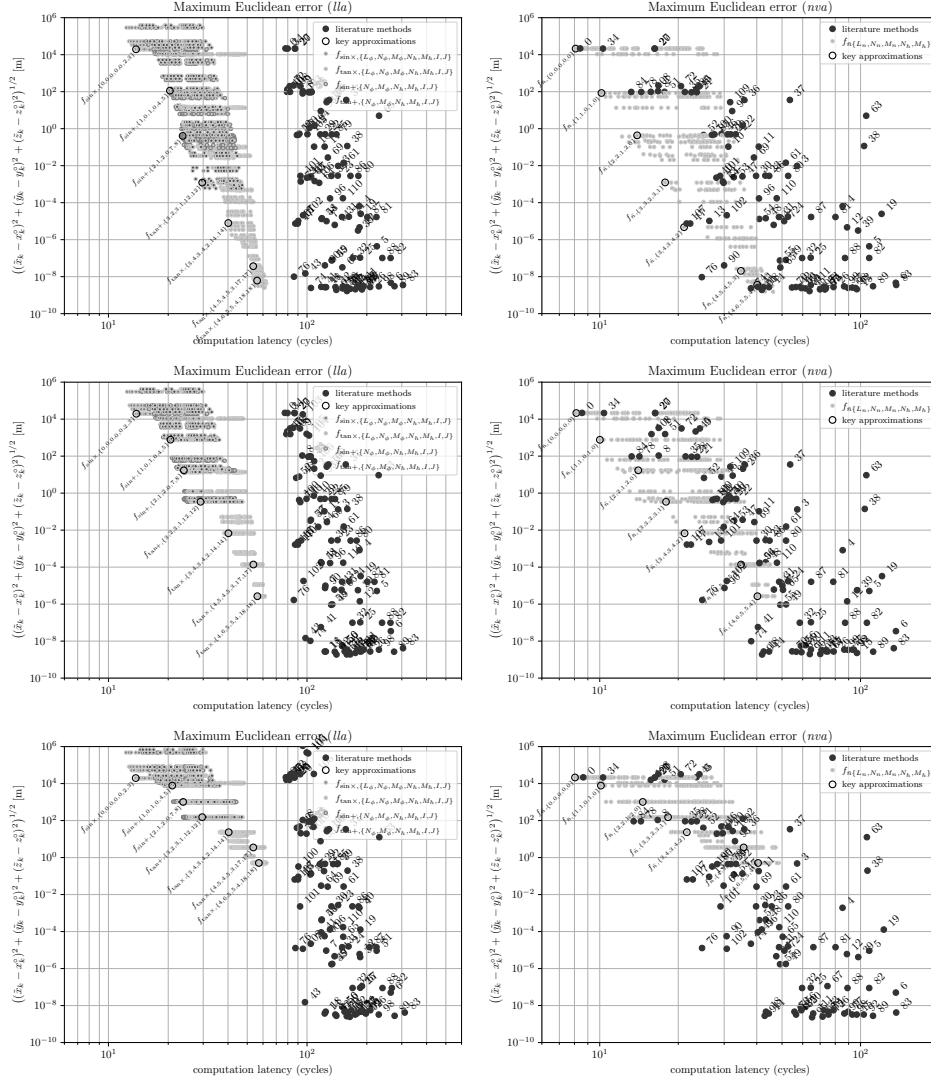
FIGURE 5. Euclidean error for the altitude ranges $[-5000, 32\,000]$m, $[-5000, 500\,000]$m and $[-5000, 5\,000\,000]$m. Comparing the Euclidean errors for the altitude range $[-5000, 100\,000]$m shown in Fig. 1 with those for the ranges $[-5000, 32\,000]$m, $[-5000, 500\,000]$m, the overall picture is the same but, for the range $[-5000, 5\,000\,000]$m, the polynomial methods (with single polynomials over the complete range) becomes inefficient and perform poorly. Note that some methods have numerical problems at very large altitudes *Ward 2020* and that the method by *Hmam 2018* performs surprisingly well for large ranges.

- All altitude error results presented in *Ligas and Banasik 2011*, except those of *Heiskanen and Moritz 1967*, appear to be off by a factor 1000. From comments in the code from *Ward 2020*, others appear to have hade the same experience. The results are included in the plot corrected for this.
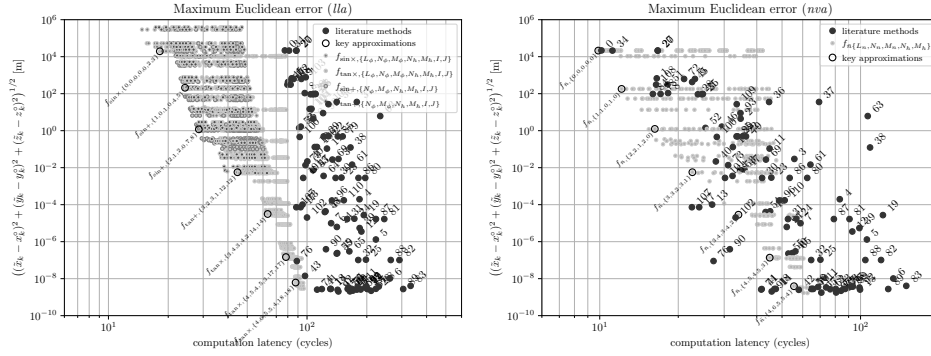
FIGURE 6. Euclidean errors for the altitude range $[-5000, 100\,000]$m all methods compiled without AVX support (compiler flag `-mno-avx`). The error results are essentially identical but the latency results are worse, especially for the polynomial methods, i.e. the polynomial methods can to a large extent be vectorized and the lack of SIMD operations favor other methods. However, SIMD instructions have been prevalent in CPUs for more than a decade and CPUs without SIMD might have different arithmetic performance profiles. Therefore, too certain conclusions should not be drawn from these results.

- Altitude error results presented in *Ligas and Banasik 2011* of *Heiskanen and Moritz 1967* are roughly a factor of 8 off. There is no obvious explanation for this and the results have been excluded not to bloat the plot.
- Results presented in *Ligas and Banasik 2011* of *Fukushima 1999* appear to have one more iteration than stated. The results are plotted against the apparent correct number of iterations in the plots.
- Multiple error results for *Borkowski 1987* are considerably higher. This is likely because the presented benchmarks ignore or miss the poor performance of the method very close to the poles.
- Methods by *Sampson 1982* adapted in *Claessens 2019* have a considerably lower performance than expected. Code is provided so likely something is wrong in the original description.

Other small variations can be explained by slight implementation differences and the sampling not capturing the largest errors. Altogether, this provides an additional confidence in the error measurements.

APPENDIX F. SOME MORE COMMENTS ABOUT THE BENCHMARK

The intention of this paper is *not* to be a review and benchmark of methods for ECEF to geodetic coordinate transformations. Hence, it is rather brief when it comes to benchmark details. Nonetheless, it contains the most extensive published benchmark of said methods which makes the benchmark valuable in itself, and due to the scarcity of benchmarks in the literature, some further comments about the benchmark are appropriate:
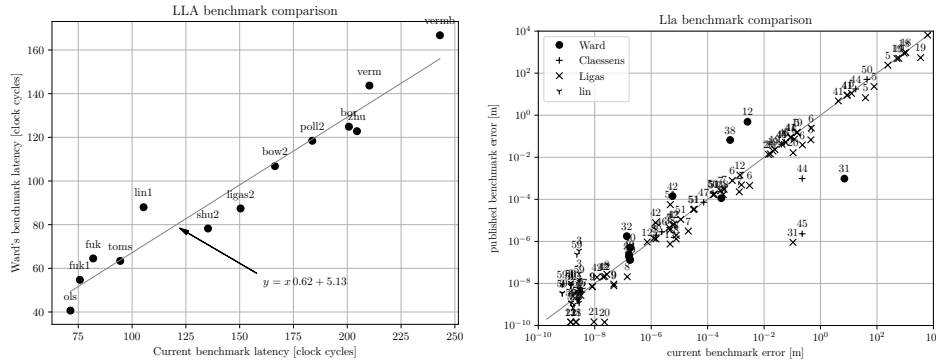
FIGURE 7. Latency measurement comparison of the current benchmark and latency measurements for *Ward 2020*. The latency measurements are not those of the article but rather the latest measurements retrieved from `https://github.com/planet36/ecef-geodetic` at 2023-12-11. Further, a latency of atan2 of 75 clock cycles has been subtracted from the latency measurements of the current benchmark to compensate for longitude not being computed. A least squares fit line is also shown.

- The benchmark methods have been selected from a combination of commonly cited methods and methods with expected good performance. From *Nilsson 2024*, it can clearly be seen not to be an exhaustive set. However, common methods are included. Poorly described methods without a clear implementation have been excluded. For example, the promising method *Turner 2009* is lacking some coefficients. I hope I am doing better.
- Micro-benchmarking on modern superscalar CPUs with modern compilers is challenging to say the least. To mention a few challenges:
  - Different cores typically provide different performance. Scheduling is correlated over at least seconds. Hence, just looping over benchmark methods from first to last will not give stable results. Rather the benchmarks methods will have to be looped over multiple times and results aggregated. Here 100 loops over the benchmark methods are used.
  - Many modern CPUs have dynamic frequency scaling. This makes latency measurements sensitive in terms of time dependent on the thermal and power supply state of the CPU and make conversion to clock cycles more difficult. Further, some instructions like AVX may be more impacted than others.
  - To avoid branch prediction, the provided data have to be unpredictably drawn from a pre-generated set. Unfortunately, to make it unpredictable, the base set may not fit in the L1 cache which will introduce infrequent L2 fetch latencies of 10 clock cycles. So the data set will have to be large enough but not too large to introduce significant L2/L3 cache misses and the sample drawing has to be randomly generated at runtime to avoid the compiler seeing through it. Here $2^{14} = 16384$ base samples with randomly shuffled indices to retrieve them have been used.

- Regular CPU clocks have a typical accuracies of tenth to hundreds of ns, roughly the time of a transformation. This means sets of transformations has to be measured. On the other hand, these measurement sets cannot be too large since then system interruption may corrupt a large portion of the measurements. Here measurement sets of 1000 samples repeated 10 000 times (with different samples) for every benchmark methods loop have been used.
    - Modern compilers are very good at removing unused code and it may interleave multiple transformations. To avoid this, some benchmark loop logic need to be made dependent on the result. We have used the micro benchmarking framework `Nanobench` *Leitner-Ankerl 2022* to handle this. Coding your own benchmark harness is a challenging task. Don't do it!
- Many iterative methods only require one or a handful of iterations to reach numerical accuracy for reasonable altitude ranges. Iterating such methods until convergence, rather than a fixed number of iterations, possibly dependent on p, will incur a significantly higher computational cost. Iterating until convergence and using an altitude range tuned for the convergence of a particular method is a good way to make that method appear better than all other methods. This is a common trap to fall into *Claessens 2007*. Don't iterate until convergence when benchmarking!
- Clearly, different transformation methods do demonstrate different accuracies, both in terms of absolute Euclidean error and in terms of different latitude and altitude errors, and applications do have varying accuracy requirements. Hence, the accuracy has to be taken into account when comparing the computational cost of methods. Further, since the relation between computational cost and latency is roughly logarithmic, it should be plotted in logarithmic scale. Interpreting just commonly provided tabulated values is hard!
- Comparing *lla* and *nva* coordinate transformations, as noted, it can be seen that *lla* methods are dominated by the evaluation of inverse trigonometric functions. This means that the core computational cost of methods are mixed by less relevant common components. As a result, *nva* versions should preferably be compared.
- Standard library trigonometric functions are typically implemented with some lookup tables. This means that they are cache sensitive. Consequently, different sample orders can give significantly different performance values. The same goes for branch-prediction, as discussed above, which to a lesser extent can affect values. As a result, one has to be very clear on what and in what order samples are provided to the methods, and simply be aware of that the results will depend on how the benchmarking is done, which is another reason to favor *nva* methods.
- Longitude has a singularity at the poles, which is another reason for favoring comparison of the n-vector versions. However, in practice, this is of less concern when using double precision. First, the likelihood of randomly sampling a problematic point is minimal (the pole would naturally be sampled with quasi-random sequences but $\mathrm{atan2}(0,0)$ is well defined for most implementations). Second, the problem is inherent to longitude and can

trivially be solved by simply ignoring samples too close to the poles. On the other hand, some methods have poor latitude accuracy at the poles, see e.g. *Fukushima 1999*, and some methods demonstrate narrow maximum error peaks at other points, see e.g. *Osen 2017*. Hence, when benchmarking with respect to maximum error, pure random or quasi-random sampling cannot be used but some points will have to be manually identified and added.

- It may appear surprising that the accuracy for longitude vary between methods. This is probably because the C standard (since C99) allows floating point contraction, see Section 6.5 of *ISO 2011*. GCC enables contraction by default and different contractions will result in different numerical results which is manifested in different maximum errors. These differences are of little practical importance but it demonstrates to what length the compiler goes to optimize the compiled methods. Consequently, benchmarking should be done in some low level language such as C/C++ and one has to be clear on the compiler and compiler options.

Few, if any, benchmarks found in the literature comes close to considering the above points. See Appendix E for some more comments.

Appendix G. Labelled approximations

In the following Table 5 to Table 7, the polynomials of the key approximations, labeled in the result plots, are provided.

$$
\begin{aligned}
\sigma_0(d) &= 9.9999716626081590 \cdot 10^{-1} \\
\sigma_1(d) &= 9.9999716626081590 \cdot 10^{-1} \\
\sigma_2(d) &= 9.9999999999933083 \cdot 10^{-1} - 4.9999952770986831 \cdot 10^{-1} d \\
\sigma_3(d) &= 9.9999999999933083 \cdot 10^{-1} - 4.9999952770986831 \cdot 10^{-1} d \\
\sigma_4(d) &= 1.0000000000000000 - 4.9999999999989962 \cdot 10^{-1} d + 4.1666643052156936 \cdot 10^{-2} d^2 \\
\tau_0(w, d) &= 0.0 \\
\tau_1(w, d) &= w 9.9999905541991507 \cdot 10^{-1} \\
\tau_2(w, d) &= w 9.9999905541991507 \cdot 10^{-1} \\
\tau_3(w, d) &= w (9.9999999999986617 \cdot 10^{-1} - 1.6666657220863013 \cdot 10^{-1} d) \\
\tau_4(w, d) &= w (9.9999999999986617 \cdot 10^{-1} - 1.6666657220863013 \cdot 10^{-1} d)
\end{aligned}
$$

TABLE 5. Approximation polynomials of labelled ECEF to geodetic coordinate approximations as implemented with Estrin. The coefficients are computed for $h \in [-5000, 100\,000]$ and $h_0 = 0$.

$\mu_{0,0}(u,v) = -6367431.3222291581 + u$

$\mu_{1,0}(u,v) = -6378123.6318397466 + u + 21384.619221178389v$

$\mu_{2,0}(u,v) = -6378136.9666263694 + u + 21491.297514157781v - 106.67829297939183v^2$

$\mu_{3,1}(u,v) = -6378136.9994595172 + 0.99999999993245003u + (21635.897371183597$
$\quad -2.2448844415581047 \cdot 10^{-5}u)v + (-255.12110929990945 + 2.2892370728809709 \cdot 10^{-5}u$
$\quad +(3.9094878910461248 - 4.4352564908397368 \cdot 10^{-7}u)v)v^2$

$\mu_{4,2}(u,v) = -6378136.9999909624 + 0.99999999999763889u + 1.5802065572606207 \cdot 10^{-19}u^2$
$\quad +(21780.894277501458 - 6.7654346288251749 \cdot 10^{-5}u + 3.523327586518059 \cdot 10^{-12}u^2)v$
$\quad +(-405.06255735505755 + 6.9626677884681548 \cdot 10^{-5}u - 3.6418186823541659 \cdot 10^{-12}u^2$
$\quad +(9.0523504657800462 - 2.0213005835652036 \cdot 10^{-6}u + 1.2163741069533121 \cdot 10^{-13}u^2)v)v^2$
$\quad +(-0.19833376155550902 + 4.897368096169858 \cdot 10^{-8}u - 3.1466289533477168 \cdot 10^{-15}u^2)v^4$

$\mu_{5,3}(u,v) = -6378136.999999837 + 0.99999999999993427u + (9.0086894408412461 \cdot 10^{-21}$
$\quad -4.1721771358431153 \cdot 10^{-28}u)u^2 + (21926.846232683445 - 0.0001359137163728073u$
$\quad +(1.4164341421699455 \cdot 10^{-11} - 5.529324196314687 \cdot 10^{-19}u)u^2)v + (-557.90712954128696$
$\quad +0.0001411089761651272u + (-1.4785186246301743 \cdot 10^{-11} + 5.7903314015836112 \cdot 10^{-19}u)u^2$
$\quad +(16.200215643865732 - 5.3621764869014012 \cdot 10^{-6}u + (6.4221743608384831 \cdot 10^{-13}$
$\quad -2.704152420119277910^{-20}u)u^2)v)v^2 + (-0.46569261099818271 + 1.7163926304246266 \cdot 10^{-7}u$
$\quad +(-2.2001911719684914 \cdot 10^{-14} + 9.6932580539601789 \cdot 10^{-22}u)u^2 + (0.01212864332278238$
$\quad -4.7225675478058751 \cdot 10^{-9}u + (6.2930011258784072 \cdot 10^{-16} - 2.8522125189628692 \cdot 10^{-23}u)u^2)v)v^4$

$\mu_{5,4}(u,v) = -6378136.9999995893 + 0.99999999999977973u + (4.5142727491369904 \cdot 10^{-20}$
$\quad -4.1725151386930229 \cdot 10^{-27}u)u^2 + 1.4635120955670929 \cdot 10^{-34}u^4 + (22073.775734502189$
$\quad -0.00022753572483565161u + (3.5589046523527045 \cdot 10^{-11} - 2.7795229385686731 \cdot 10^{-18}u)u^2$
$\quad +8.6774096768703165 \cdot 10^{-26}u^4)v + (-713.77257463984938 + 0.00023830325013161956u$
$\quad +(-3.7512900428756296 \cdot 10^{-11} + 2.9410407690609742 \cdot 10^{-18}u)u^2 - 9.2051543802841124 \cdot 10^{-26}u^4$
$\quad +(25.535665117187818 - 1.1183565979926647 \cdot 10^{-5}u + (2.0034813315984979 \cdot 10^{-12}$
$\quad -1.6851285921853015 \cdot 10^{-19}u)u^2 + 5.5133913606023886 \cdot 10^{-27}u^4)v)v^2 + (-0.87962551332934436$
$\quad +4.2975946940615239 \cdot 10^{-7}u + (-8.2360392773041159 \cdot 10^{-14} + 7.2421780503870395 \cdot 10^{-21}u)u^2$
$\quad -2.4446464398246533 \cdot 10^{-28}u^4 + (0.026555348121184361 - 1.3718782035050124 \cdot 10^{-8}u$
$\quad +(2.7329656904472876 \cdot 10^{-15} - 2.4714925716231548 \cdot 10^{-22}u)u^2 + 8.5203151372608724 \cdot 10^{-30}u^4)v)v^4$

$\omega_{0,0}(u,v) = 0.0$

$\omega_{1,0}(u,v) = 0.0066677813753770136$

$\omega_{2,1}(u,v) = 0.013446184736230014 - 1.0515236264437181 \cdot 10^{-9}u + (-0.00022196483792195034$
$\quad +2.4231357903357331 \cdot 10^{-11}u)v$

$\omega_{3,2}(u,v) = 0.02023800884030541 - 3.1689947923483929 \cdot 10^{-9}u + 1.6503606600562022 \cdot 10^{-16}u^2$
$\quad +(-0.0004785600602124579 + 1.0339367946779417 \cdot 10^{-10}u - 6.1276159848868637 \cdot 10^{-18}u^2)v$
$\quad +(1.2255186842036269 \cdot 10^{-5} - 2.9789880393313049 \cdot 10^{-12}u + 1.8956055600526669 \cdot 10^{-19}u^2)v^2$

$\omega_{4,3}(u,v) = 0.027074537946419158 - 6.3663290353834142 \cdot 10^{-9}u + (6.6347135933514977 \cdot 10^{-16}$
$\quad -2.5899885739079588 \cdot 10^{-23}u)u^2 + (-0.00082614540139308665 + 2.6591180000141378 \cdot 10^{-10}u$
$\quad +(-3.1458081288862306 \cdot 10^{-17} + 1.3160531764922644 \cdot 10^{-24}u)u^2)v + (2.7326402303242933 \cdot 10^{-5}$
$\quad -9.9255846855924077 \cdot 10^{-12}u + (1.2611748377621174 \cdot 10^{-18} - 5.524714330136761 \cdot 10^{-26}u)u^2$
$\quad +(-8.3406214314548869 \cdot 10^{-7} + 3.2207409051958092 \cdot 10^{-13}u + (-4.2673520748401045 \cdot 10^{-20}$
$\quad +1.9262444612240382 \cdot 10^{-27}u)u^2)v)v^2$

$\omega_{5,4}(u,v) = 0.033956858269743512 - 1.0657992633478044 \cdot 10^{-8}u + (1.6670252730549704 \cdot 10^{-15}$
$\quad -1.3019553810283226 \cdot 10^{-22}u)u^2 + 4.0645825278533089 \cdot 10^{-30}u^4 + (-0.0012704734728483523$
$\quad +5.4298359021842561 \cdot 10^{-10}u + (-9.6247756886895796 \cdot 10^{-17} + 8.0493882503509578 \cdot 10^{-24}u)u^2$
$\quad -2.6240930039793388 \cdot 10^{-31}u^4)v + (5.0407946329043319 \cdot 10^{-5} - 2.4311236288225156 \cdot 10^{-11}u$
$\quad +(4.6237683172662731 \cdot 10^{-18} - 4.046026381146591 \cdot 10^{-25}u)u^2 + 1.3611682445895033 \cdot 10^{-32}u^4$
$\quad +(-1.9142270212250502 \cdot 10^{-6} + 9.8416784098310913 \cdot 10^{-13}u + (-1.9547420630659842 \cdot 10^{-19}$
$\quad +1.7642687942146882 \cdot 10^{-26}u)u^2 - 6.074031842567329 \cdot 10^{-34}u^4)v)v^2 + (6.3806316097197935 \cdot 10^{-8}$
$\quad -3.4050334493087929 \cdot 10^{-14}u + (6.9509879641250328 \cdot 10^{-21} - 6.4057707012819846 \cdot 10^{-28}u)u^2$
$\quad +2.2416300605419168 \cdot 10^{-35}u^4)v^4$

$\omega_{6,5}(u,v) = 0.040885295839059019 - 1.6058512798514048 \cdot 10^{-8}u + (3.3508256373764818 \cdot 10^{-15}$
$\quad -3.926840751433145 \cdot 10^{-22}u)u^2 + (2.452407337947089 \cdot 10^{-29} - 6.3787271347333624 \cdot 10^{-37}u)u^4$
$\quad +(-0.0018135837610434001 + 9.6632292183719524 \cdot 10^{-10}u + (-2.2823864407320369 \cdot 10^{-16}$
$\quad +2.8625533791616239 \cdot 10^{-23}u)u^2 + (-1.8662042533586911 \cdot 10^{-30} + 5.0002116900156677 \cdot 10^{-38}u)u^4)v$
$\quad +(8.3959005641911052 \cdot 10^{-5} - 5.0462939089357817 \cdot 10^{-11}u + (1.2777379582642763 \cdot 10^{-17}$
$\quad -1.6756621695205854 \cdot 10^{-24}u)u^2 + (1.1268286476356885 \cdot 10^{-31} - 3.0887598999489422 \cdot 10^{-39}u)u^4$
$\quad +(-3.6754339736361957 \cdot 10^{-6} + 2.3558477370497502 \cdot 10^{-12}u + (-6.2286650409724249 \cdot 10^{-19}$
$\quad +8.423442141937836610^{-26}u)u^2 + (-5.795633529300024310^{-33} + 1.6169761725178128 \cdot 10^{-40}u)u^4)v)v^2$
$\quad +(1.5042738265816568 \cdot 10^{-7} - 1.0030850101437109 \cdot 10^{-13}u + (2.7300583918580043 \cdot 10^{-20}$
$\quad -3.7741601218646458 \cdot 10^{-27}u)u^2 + (2.6418278049580857 \cdot 10^{-34} - 7.473104708913223 \cdot 10^{-42}u)u^4$
$\quad +(-5.2615868937848073 \cdot 10^{-9} + 3.5969760005163239 \cdot 10^{-15}u + (-9.9797774889619664 \cdot 10^{-22}$
$\quad +1.4008066097662379 \cdot 10^{-28}u)u^2 + (-9.926763165672736 \cdot 10^{-36} + 2.8366680915535596 \cdot 10^{-43}u)u^4)v)v^4$

TABLE 6. Approximation polynomials of labeled ECEF to geodetic coordinate approximations as implemented with Estrin. The coefficients are computed for $h \in [-5000, 100\,000]$ and $h_0 = 0$.

$\xi_3(x) = x(9.9535795470534027 \cdot 10^1 - 2.8869023791774234 \cdot 10^1 x^2 + 7.9339041370619872 \cdot 10^2 x^4)$

$\xi_5(x) = x(9.9986632904710004 \cdot 10^1 - 3.3030478126799267 \cdot 10^1 x^2 + (1.8015928178377459 \cdot 10^1$
$\quad - 8.5156335459610334 \cdot 10^2 x^2)x^4 + 2.0845107810858079 \cdot 10^2 x^8)$

$\xi_8(x) = x(9.9999933557895379 \cdot 10^1 - 3.3329860785866898 \cdot 10^1 x^2 + (1.9946565664948636 \cdot 10^1$
$\quad - 1.3908629610769453 \cdot 10^1 x^2)x^4 + (9.6421974777848821 \cdot 10^2 - 5.5912328807716874 \cdot 10^2 x^2$
$\quad + (2.1862959296299865 \cdot 10^2 - 4.0545676075818409 \cdot 10^3 x^2)x^4)x^8)$

$\xi_{12}(x) = x(9.9999999943022189 \cdot 10^1 - 3.3333327040718965 \cdot 10^1 x^2 + (1.9999793539915971 \cdot 10^1$
$\quad - 1.4282551389892477 \cdot 10^1 x^2)x^4 + (1.1083671099533618 \cdot 10^1 - 8.9411184337301530 \cdot 10^2 x^2$
$\quad + (7.1430746289771899 \cdot 10^2 - 5.2514556999956749 \cdot 10^2 x^2)x^4)x^8 + (3.2232566609514774 \cdot 10^2$
$\quad - 1.4721216068835910 \cdot 10^2 x^2 + (4.2936462844677191 \cdot 10^3 - 5.8769992093623553 \cdot 10^4 x^2)x^4)x^{16})$

$\xi_{14}(x) = x(9.9999999998328136 \cdot 10^1 - 3.3333333086677668 \cdot 10^1 x^2 + (1.9999989164783083 \cdot 10^1$
$\quad - 1.4285491033770566 \cdot 10^1 x^2)x^4 + (1.1108488389521914 \cdot 10^1 - 9.0713495063830683 \cdot 10^2 x^2$
$\quad + (7.5933101852628750 \cdot 10^2 - 6.3109521418777435 \cdot 10^2 x^2)x^4)x^8 + (4.9445357766039380 \cdot 10^2$
$\quad - 3.3981220148545598 \cdot 10^2 x^2 + (1.8820607710988513 \cdot 10^2 - 7.6115686823698953 \cdot 10^3 x^2)x^4$
$\quad + (1.9542989485087399 \cdot 10^3 - 2.3593188960412083 \cdot 10^4 x^2)x^8)x^{16})$

$\xi_{17}(x) = x(9.9999999999991586 \cdot 10^1 - 3.3333333331539649 \cdot 10^1 x^2 + (1.9999999885901307 \cdot 10^1$
$\quad - 1.4285710866597597 \cdot 10^1 x^2)x^4 + (1.1111052308663949 \cdot 10^1 - 9.0902614649300906 \cdot 10^2 x^2$
$\quad + (7.6874146803011537 \cdot 10^2 - 6.6400996804419749 \cdot 10^2 x^2)x^4)x^8 + (5.7751981894433748 \cdot 10^2$
$\quad - 4.9340121701547388 \cdot 10^2 x^2 + (3.9762413378979828 \cdot 10^2 - 2.8629853703447561 \cdot 10^2 x^2)x^4$
$\quad + (1.7310365496208254 \cdot 10^2 - 8.2096187905995513 \cdot 10^3 x^2 + (2.8093457170694520 \cdot 10^3$
$\quad - 6.0940031581488599 \cdot 10^4 x^2)x^4)x^8)x^{16} + 6.2436108681934464 \cdot 10^5 x^{32})$

$\xi_{18}(x) = x(9.9999999999998558 \cdot 10^1 - 3.3333333332990472 \cdot 10^1 x^2 + (1.9999999975665970 \cdot 10^1$
$\quad - 1.4285713471275124 \cdot 10^1 x^2)x^4 + (1.1111095442381502 \cdot 10^1 - 9.0907156394328137 \cdot 10^2 x^2$
$\quad + (7.6906649156526998 \cdot 10^2 - 6.6566100086412207 \cdot 10^2 x^2)x^4)x^8 + (5.8364603332581473 \cdot 10^2$
$\quad - 5.1030977240766378 \cdot 10^2 x^2 + (4.3267805093829844 \cdot 10^2 - 3.4100063401437874 \cdot 10^2 x^2)x^4$
$\quad + (2.3697852281270090 \cdot 10^2 - 1.3702546920513891 \cdot 10^2 x^2 + (6.1837955998122361 \cdot 10^3$
$\quad - 2.0101395373502504 \cdot 10^3 x^2)x^4)x^8)x^{16} + (4.1436296328711983 \cdot 10^4 - 4.0407586855442829 \cdot 10^5 x^2)x^{32})$

$\chi_2(x) = 1.5702116976458603 - 2.0212058400388336 \cdot 10^1 x + 4.6707077880155363 \cdot 10^2 x^2$

$\chi_4(x) = 1.5707878616372565 - 2.1412466400217967 \cdot 10^1 x + (8.4666692360295800 \cdot 10^2$
$\quad - 3.5756539685967685 \cdot 10^2 x)x^2 + 8.6486772213302613 \cdot 10^3 x^4$

$\chi_7(x) = 1.5707963049952714 - 2.1459880383418343 \cdot 10^1 x + (8.8979049893930584 \cdot 10^2$
$\quad - 5.0174715212327148 \cdot 10^2 x)x^2 + (3.0893053197591073 \cdot 10^2 - 1.7089810809721586 \cdot 10^2 x$
$\quad + (6.6712932596193130 \cdot 10^3 - 1.2628309167103800 \cdot 10^3 x^2)x^2)x^4$

$\chi_{12}(x) = 1.5707963267933006 - 2.1460183603240527 \cdot 10^1 x + (8.9048588758505052 \cdot 10^2$
$\quad - 5.0792024609074237 \cdot 10^2 x)x^2 + (3.3671622816568150 \cdot 10^2 - 2.4303153862137010 \cdot 10^2 x$
$\quad + (1.8329796462243492 \cdot 10^2 - 1.3751038185856593 \cdot 10^2 x^2)x^4 + (9.5272136428286426 \cdot 10^3$
$\quad - 5.5320203601637119 \cdot 10^3 x + (2.4008869075915833 \cdot 10^3 - 6.6857373783667137 \cdot 10^4 x^2)x^2$
$\quad + 8.7773781127018793 \cdot 10^5 x^4)x^8$

$\chi_{14}(x) = 1.5707963267948586 - 2.1460183658456538 \cdot 10^1 x + (8.9048621136695723 \cdot 10^2$
$\quad - 5.0792770716881518 \cdot 10^2 x)x^2 + (3.3680571282738509 \cdot 10^2 - 2.4367246446961202 \cdot 10^2 x$
$\quad + (1.8626098028204800 \cdot 10^2 - 1.4676637467188599 \cdot 10^2 x)x^2)x^4 + (1.1531109639172660 \cdot 10^2$
$\quad - 8.5675083245346239 \cdot 10^3 x + (5.6003920887711281 \cdot 10^3 - 2.9601736597984054 \cdot 10^3 x)x^2$
$\quad + (1.1466969584531041 \cdot 10^3 - 2.8304614323065713 \cdot 10^4 x + 3.2965787399023498 \cdot 10^5 x^2)x^4)x^8$

$\chi_{17}(x) = 1.5707963267948965 - 2.1460183660245246 \cdot 10^1 x + (8.9048622536943916 \cdot 10^2$
$\quad - 5.0792814046672612 \cdot 10^2 x)x^2 + (3.3681275570828086 \cdot 10^2 - 2.4374172925348297 \cdot 10^2 x$
$\quad + (1.8670862830280291 \cdot 10^2 - 1.4876918953706647 \cdot 10^2 x)x^2)x^4 + (1.2172747383436669 \cdot 10^2$
$\quad - 1.0071291531222582 \cdot 10^2 x + (8.2100842886296591 \cdot 10^3 - 6.3278993837482987 \cdot 10^3 x)x^2$
$\quad + (4.3671279910859448 \cdot 10^3 - 2.5369588366614161 \cdot 10^3 x + (1.1590307122361844 \cdot 10^3$
$\quad - 3.8309521446820528 \cdot 10^4 x)x^2)x^4)x^8 + (8.0476117495016973 \cdot 10^5 - 8.0043584568231787 \cdot 10^6 x)x^{16}$

$\chi_{18}(x) = 1.5707963267948966 - 2.1460183660253421 \cdot 10^1 x + (8.9048622545903351 \cdot 10^2$
$\quad - 5.0792814434974340 \cdot 10^2 x)x^2 + (3.3681284430401487 \cdot 10^2 - 2.4374295730838710 \cdot 10^2 x$
$\quad + (1.8671988159799984 \cdot 10^2 - 1.4884115235275848 \cdot 10^2 x)x^2)x^4 + (1.2206039463975348 \cdot 10^2$
$\quad - 1.0185410804411290 \cdot 10^2 x + (8.5042859077692046 \cdot 10^3 - 6.9026076875376219 \cdot 10^3 x)x^2$
$\quad + (5.2181956820067259 \cdot 10^3 - 3.4855347796590377 \cdot 10^3 x + (1.9414549204238104 \cdot 10^3$
$\quad - 8.4603434241738747 \cdot 10^4 x)x^2)x^4)x^8 + (2.6620763505161977 \cdot 10^4 - 5.3242183459453063 \cdot 10^5 x$
$\quad + 5.0486339748452772 \cdot 10^6 x^2)x^{16}$

TABLE 7. Inverse trigonometric function approximation polynomials of labeled ECEF to geodetic coordinate (lla) approximations as implemented with Estrin.